September 2020

Historical Changes in Planform Geometry of the Amite and Comite Rivers and Implications on Flood Routing

Kathleen E. Harris
Louisiana State University and Agricultural and Mechanical College

HISTORICAL CHANGES IN PLANFORM GEOMETRY OF THE AMITE AND COMITE RIVERS AND IMPLICATIONS ON FLOOD ROUTING

A Thesis

Submitted to the Graduate Faculty of the
Louisiana State University and
Agricultural and Mechanical College
in partial fulfillment of the
requirements for the degree of
Master of Science

in

The Department of Civil and Environmental Engineering

by
Kathleen Eubanks Harris
B.S. Texas A&M University, 2016
December 2020

ACKNOWLEDGMENTS

First, I would like to thank my advisor Dr. Clint Willson for his sound guidance and unwavering support. I would also like to thank my committee members, Dr. Robert Twilley, Dr. Kory Konsoer, and Dr. Zhiqiang Deng for their valuable input and unique perspectives. Additionally, thanks are in order to the National Academies of Sciences' Gulf Research Program and the Robert Wood Johnson Foundation, which funds the project "Inland from the Coast: A multi-scalar approach to community resilience and wellbeing." This thesis research draws on a portion of that project and the grant provided funding for my graduate work. Finally, I would like to thank my parents and sister for their unconditional love and support as I changed disciplines and embarked on graduate school, my friends for providing respite and encouragement, and my husband Brian who has been the best friend I made in graduate school and provided companionship, reassurance, comedic relief, and sound geotechnical advice throughout my graduate career.

TABLE OF CONTENTS

LIST OF TABLES

LIST OF FIGURES

ABSTRACT

The Amite River Basin is a 2,220 square-mile basin spanning from southwest Mississippi through southeast Louisiana, encompassing Baton Rouge and its suburbs. In response to historic flooding in August 2016 and other major flood events in the past several decades, the basin has been the subject of a number of studies to quantify the impacts of changes in land-use and reduction in river length and sinuosity. However, there have yet to be relationships defined between the changes in the historical river planform and the resulting flow, stages, and subsequent flood depths. River lengths and sinuosity were measured from the 1930s to present, confirming there has been an overall 6 and 13% decrease in length and sinuosity of the Comite and Amtie Rivers upstream of their confluence, respectively, from the 1930s to present. Planform geometries from four time period scenarios from the 1930's to present were input into a combined 1D/2D unsteady flow HEC-RAS model, which is run using four spatially-variable rainfall events ranging from 1- to greater than 500-year return period flows to examine the significance on flood characteristics. The results show an overall increase in flow and stage peak magnitude over time, corresponding to an overall decrease in river length and sinuosity. The impacts were largest for the 3- to 6-year return period flow event due to the magnitude and rainfall distribution of the historic event used. Results from this study will be compared to and combined with complementary projects, focused on spatial and temporal changes in land use and precipitation events, to better understand the driving variables impacting the stages, discharges, and subsequent flood risk within the basin. Further, this knowledge can be applied to better inform mitigation and construction projects within the basin in the future.

CHAPTER 1. INTRODUCTION

1.1. Overview

The Amite River Basin spans from southwest Mississippi through southeast Louisiana and drains into Lake Maurepas, a tidally-influenced lake that connects to the Gulf of Mexico, by way of Lake Pontchartrain. The Amite and Comite Rivers serve as the main arteries within the basin, and the portions of these two rivers within Louisiana will be the focus of this study (Figure 1). The drainage area is approximated to be 2,220 square miles (Hood, Patrick, & Corcoran, 2007). The Amite River Basin is predominately rural aside from the metropolitan area of Baton Rouge and the surrounding suburban communities in the mid to lower basin, an area which has seen accelerated population growth and land use change since the 1960s (Gulf Engineers and Consultants, 2015). Sand and gravel mining along the Amite and Comite Rivers is another driver of change within the basin that has caused river shortening and straightening by pit capture, changes in sediment yield, and incision and head cutting. The mining is spatially concentrated in the middle portion of the basin, with mining activity peaking in the 1970s (Hood, Patrick, & Corcoran, 2007). This basin has been subject to several notable flood events since development, including April 1977 and April 1983, and most recently by record rainfall in August 2016 that resulted in unprecedented flooding across Baton Rouge and its surrounding areas. The August 2016 rainfall event was caused by a slow-moving, low pressure, high atmospheric moisture system that moved across southern Mississippi and Louisiana (Watson et al., 2017). Approximately 21.9 inches of rain in Livingston, LA and 31.4 inches in Watson, LA were reported for the 48-hr rainfall accumulation, with the latter breaking the greatest 48-hr rainfall record in Louisiana (Brown et al., 2020). The rainfall resulted in 13 immediate fatalities and $10.4 billion of damage to more than 140,000 homes (Watson et al., 2017). The subsequent recording-breaking flooding within the

Amite River Basin raised concerns of whether the rapid development in the basin and the historic sand and gravel mining negatively impacted flooding hazard in the basin.

Figure 1. Amite River Basin in Louisiana and Mississippi shown with parish and county boundaries.

1.2. Research objectives

The objective of this thesis is to document and quantify the changes in length and sinuosity of both the Amite and Comite Rivers and examine the impact of these changes on the planform geometry and the resulting flows, stages, and flow attenuation. Other research is currently being conducted documenting and quantifying the changes in land uses and precipitations events within the basin over time. Related and future work will use the results from this thesis to isolate these variables and derive relationships between land use, stream characteristics, and precipitation

events and how these changes have impacted river flows, stages, and subsequent flood inundation depths in the basin.

Specifically, this study will address the following questions:

- How have the Amite and Comite Rivers changed in length and sinuosity over the past 90 years?
- Is there a relationship between the planform geometry changes of the Amite and Comite rivers and the flows, stages, and peak attenuation along the rivers?
- If flows and stages are sensitive to the changes in length and sinuosity as a results of changes in planform geometry, under what flow events are the effects most apparent?

1.3. Thesis outline

This thesis will first introduce the study area, study motivation, and resulting research questions. A literature review is provided summarizing relevant studies on how disturbances in the basin are expected to impact the river flow and depths. Next, the methodology for collecting historical river planform geometry is presented, followed by details on the model used, sensitivity analyses performed, and the methods used to modify the model for the study. Results for both the geospatial investigation of historic planform changes in the basin and the model scenarios are then presented. The conclusion then discusses the results and their implications, in addition to ongoing research utilizing this work.

CHAPTER 2. LITERATURE REVIEW

2.1. Amite River Basin study area background and development

Before modern settlement, the Amite River Basin consisted mostly of mixed deciduous and evergreen forests, with small patches of prairie in the current East Baton Rouge Parish. Since its development, the land use has transformed into mining areas, managed forest, pastures, and developed communities (Autin, 1992). Steady population increase has been seen within the basin since the 1930s, stimulated by the expansion of the state government, growing universities, and the start of local refining and petrochemical industry (Gulf Engineers and Consultants, 2015). Sand and gravel mining has been a part of the basin since the early 1940s, centered around Grangeville, LA in the mid-Amite River Basin (Autin, 1992). Population growth and land-use changes in the basin were again accelerated in the 1960s, with Baton Rouge being one of the fastest growing urban areas in Louisiana (Gulf Engineers and Consultants, 2015). This time period saw urban acreage increase from 24,500 acres in 1956 to 81,400 acres in 1979 (Emmer, 2003). In the 1990s, the area experienced urban sprawl into surrounding communities, again resulting in major land-use changes. For example, the land cover within the basin increased by 50% and 30% in high intensity developed land and medium intensity development between 2001 and 2011, respectively (FEMA, 2017). Within the five main parishes that comprise the Amite River Basin, there has been around a 6% annual increase in population from 1900 to 2017 with the highest percent increase being in Livingston Parish and the lowest in East Feliciana, which has seen an overall decrease in population (Figure 2). The population of the basin by parish (Figure 1) as of 2017 was determined to be 737,219 (Table 1).

Table 1. Population data modified from GEC 2015, updated with 2017 census numbers from www.census.gov.

	1900	1920	1940	1960	1980	2000	2010	2017
East Baton Rouge	31,153	44,513	88,415	230,058	366,191	412,852	440,171	446,268
Livingston	8,100	11,643	17,790	26,974	58,806	91,814	128,026	138,228
Ascension	24,142	22,155	21,215	27,927	50,068	76,627	107,215	122,948
St. Helena	8,479	8,427	9,542	9,162	9,827	10,525	11,203	10,363
East Feliciana	20,443	17,487	18,039	20,198	19,015	21,360	20,267	19,412
Total	92,317	104,225	155,001	314,319	503,907	613,178	706,882	737,219

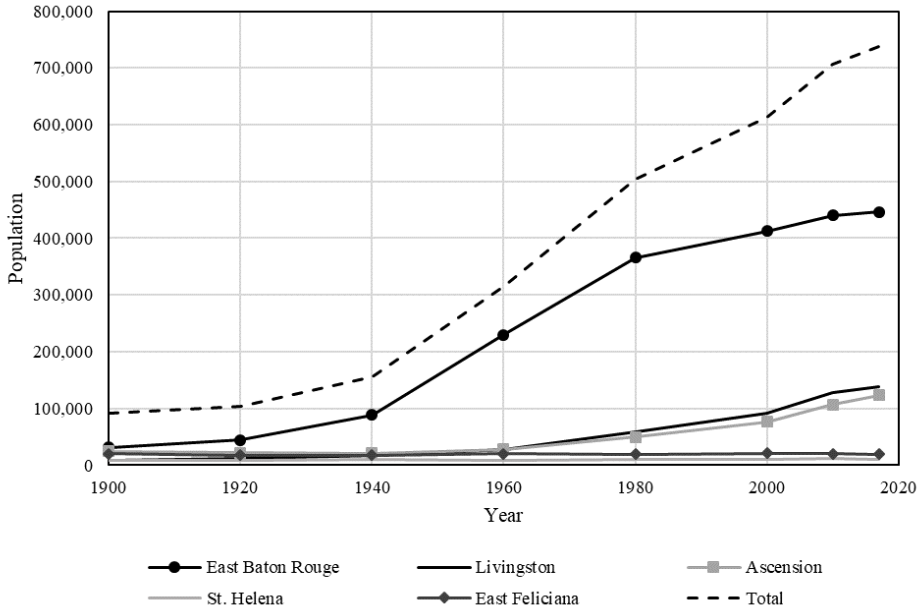

Figure 2. Population of portion of interest in the Amite River Basin 1990-2017, created with data from www.census.gov.

The rapid population growth and subsequent development of the watershed has caused significant disturbance to the Amite River. The Amite River is one of the 15 water bodies in Louisiana that is on the U.S. EPA impaired water bodies list, specifically due to sediment concentrations. The estimated average annual rate of soil erosion in the basin is approximately 13 tons per hectare, resulting in an annual nonpoint sediment concentration of 103 mg/L (Mishra & Deng, 2009). The lower Amite is also included on the impaired water list due to unsuitable concentrations of dissolved oxygen, nitrate and nitrite, chlorides, and total phosphorus (Deng & Patil, 2011). Overall, approximately 17 square miles have experienced fish and wildlife

degradations believed to be a result of urbanization, sand and gravel mining, and agricultural and forestry practices of the past 50 years (Mishra & Deng, 2009).

2.2. Sand and Gravel Activity & Impact on Flooding

The Amite River provides a model example of a disturbed coarse sand- and gravel- bed load meandering system with characteristic incised channels and flashy discharge (Autin & Fontana, 1980). The sand and gravel mining industry has been present in the basin since the 1940s with a peak in the 1970s (Hood, Patrick, & Corcoran, 2007), at which point the Amite River Basin accounted for approximately 34% of the state's total sand and gravel mining (Autin, 1992). Instream sand and gravel mining is known to alter the affected system by causing the mined reach to become incised, as well as initially reducing supplies of coarse material downstream (Step, 1999). Likewise, due to the mining pits inherent instability, they are prone to scour and depositions leading to migration of the pits, scour upstream and downstream of the disturbance, and changes in the morphology downstream by altering the overall sediment yield (Lee, Fu, & Song, 1993). In addition, the presence of open mining pits adjacent to the river results in shortening and straightening as high water events direct water into mining areas, causing cutoffs and straightening of bends similar to a natural process, but on a larger and expedited scale (Hood, Patrick, & Corcoran, 2007).

Within the Amite River, the reduction in channel length has caused an increase in channel slope and a subsequent increase in sediment transport capacity, resulting in channel incision in the upper portion of the watershed (Little, 2011). Previous research suggests decreases in channel length due to mining practices can be linked to increased downstream flood elevations, more rapid flood crests, and increased sedimentation rates, however, the impacts on flood hydrology have not been entirely quantified (Autin, 1992). However, a sensitivity analysis conducted in a hydraulic

computer model suggested that without considering changes in cross section characteristics, a 20% reduction in length in the Amite River upstream of the confluence could produce a 6 to 9.6-inch stage increase at Denham Springs (Autin, 1992). Mossa (1997) utilized photographs, maps, and other document sources to compile land cover data to compare channel change with mining activities between 1940 and 1980. This work indicated a statistical link between floodplain mining and channel change on the Amite River, showing statistically robust, moderate correlations for variable associations involving river channel migration in terms of the area between old and new channel positions as the dependent variable and the amount of area affected by mining or ponding due to mining as independent variables. In a similar study, a statistical link between floodplain mining area and channel change on the Amite River between 1976/1981 and 1998 by comparing the number and area of mines with channel area, lateral migration, and point bar area (Davis, 2009).

2.3 Impact of Channel Straightening

The idea of identifying direct and indirect human impacts on rivers is not a new concept. The recognition of land use change as an impact on river network change dates back more than a century (Marsh, 1864). In recent years, more emphasis has been placed on the impact of land use and climate change on rivers and flooding in the wake of storms leading to widespread urban flooding (Zhang et al., 2018; Yang et al., 2013). Channelization is also often cited as a direct human impact that alters rivers, but it is typically referencing hardening of the banks and creating concrete channels during development of an area (Wohl, 2006). This results in shorter, straighter reaches that also lack the natural roughness of vegetated channels. It is also established that as natural channels become straighter, steeper, and less complex, there is incision and widening in the channelized and upstream segments of the reaches and aggradation and increased overbank flooding in the downstream reaches (Schoof, 1980; Simon, 1994; Wyzga, 2001). Straightening,

deepening, and widening of the river channels also results in increased conveyance (Doyle, 2007) and subsequent increased celerity due in part to the increased slope (Campbell, Kumar, & Johnson, 1972; Wyzga, 1997). Since the flood travel time is decreased with straightening, the time an area spends flooded decreases in general (Campbell, Kumar, & Johnson, 1972). Conversely, the presence of woody debris, increased roughness due to natural banks, and the presence of meanders decreases peak flow and decreases celerity (Sholtes & Doyle, 2011). The impact developed and straightened channels would have on a flow hydrograph are shown in Figure *3*. A more developed basin with further channel straightening results in a higher, narrower hydrograph with earlier peak arrival times (Bedient, Huber, & Vieux, 2013).

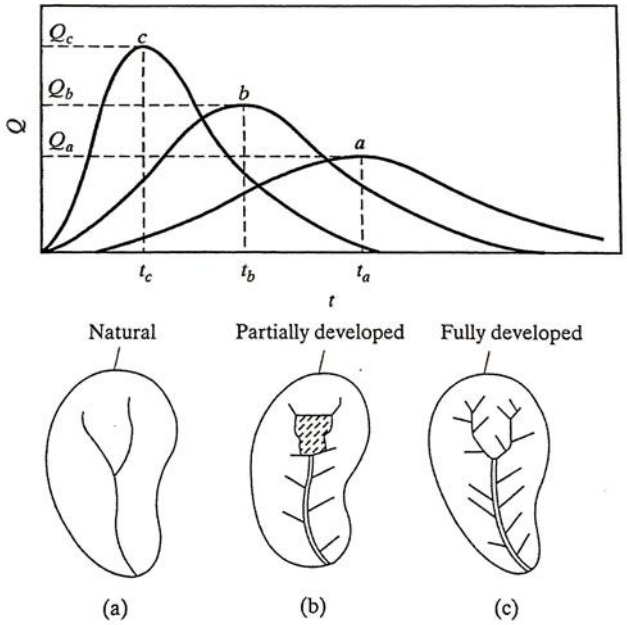

Figure 3. Impact developing a river system has on the flow hydrographs taken from Bedient, Huber, & Vieux, 2013.

These relationships are generalized cases of behaviors in response to channel change. In reality, a river system may undergo non-uniform changes in length and therefore changes in conveyance resulting from the channel changes may have additive or reductive impacts on flood celerity and magnitude.

2.4 Impact of Channel Cross Section Shape

Despite the abundance of research on how flow is impacted when channel change occurs in the form of aggradation, degradation, widening, or narrowing, there is a lack of published material focused on the impact that the channel shape alone has on flow and conveyance, given a consistent cross-sectional area. This is important to understand when recreating bathymetry to reflect historical planform geometries, such as in the case where there is a lack of historical bathymetric data. Neal et al. (2015) focused on utilizing simplified shapes, dictated by a varying shape factor, *s*, that ranged from rectangular (s = 0) to triangular (s = 1) channels. Their work is applicable for creating and calibrating large-scale hydraulic models when faced with a lack of bathymetric data. It was found that calibrating the channels with manning's roughness coefficient, *n*, was feasible and comparable, but required higher than expected or physically plausible manning's values, thus influencing the wave propagation. It was also demonstrated that the error for wetted perimeter, using the fabricated geometry, had less of an effect on the simulated levels than the error expected in real world applications (Neal et al., 2015). So, whereas cross sectional area changes due to channel morphology change are expected to greatly impact flow, varying cross section shapes alone while keeping the area consistent does not seem as likely to make a major impact on the flows and stages. In the case of this thesis work, the lengths between cross sections will be updated to reflect the historical changes, while the individual cross section geometries will be kept constant. Consequently, the impact the orientation of the cross section within a bend has on the shape is ignored. The information provided by this literature review supports this as an acceptable simplification and valid methodology.

CHAPTER 3. METHODOLOGY

3.1. Data Collection

The initial step was to measure and compare the length and sinuosity along the main stems of the Amite and Comite Rivers. The historical paths were delineated from USGS topographic maps collected from the USGS website TopoView. These maps were brought into ArcMap, converted to a consistent datum, in this case NAD83 UTM Zone 15N, and digitized (Figure *4*). Most maps were 1:24,000 or 1:62,500 scale, with a few 1:100,000 scale maps being used when higher resolution maps were unavailable. The historical maps were divided into three time periods, the 1930/40s, 1950/60s, and 1980/90s, and then compared with data from National Agriculture Imagery Program (NAIP) aerial photos from 2017, since a more recent and complete set of topographic maps were not available for the basin. The three historical time periods were chosen based on availability of data and a 20-year time frame was needed to have enough maps to cover the entire Amite and Comite Rivers. Bank lines were digitized with vertices every 250 feet and then were used to interpolate the centerline via the National Center for Earth-Surface Dynamics (NCED) channel planform statistics toolbox (Lauer, 2006).

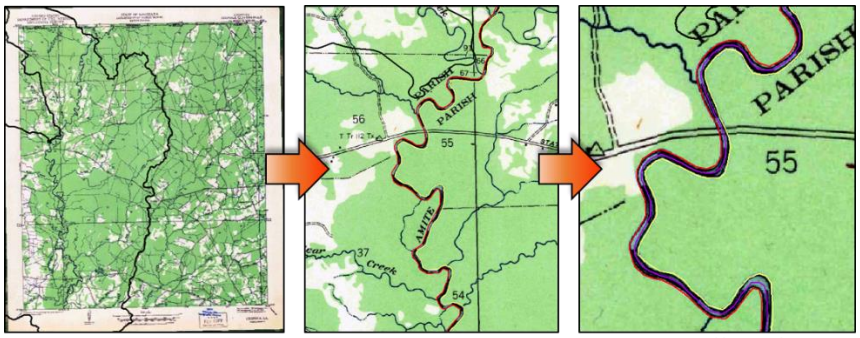

USGS Historic Topo Map | Digitize banks | Centerline via NCED tool

Figure 4. Example methods and historical topographic map from the centerline digitization process.

A potential source of error in the digitizing process is the difference in scale between the maps, causing varying levels of accuracy and the possibility of differences in the mapped features. This error is expected to be insignificant as the river lines up spatially where two maps meet so distortion between the maps of varying resolutions is not present. A more significant opportunity for error is within the few reaches that were only available in 1:100,000 scale maps where banklines had to be assumed. However, given the large scale of the study area and the lack of alternative historical bathymetry, the error introduced by the bankline assumptions is anticipated to have little impact on the project as a whole. The varying resolutions of the maps, the precision of the digitizing process, and the conversion between map projections could introduce error in the exact lengths and paths of the river reaches. Therefore, ±1% change in length and sinuosity is considered to be within the margin of error and hence insignificant. The northern-most HUC12, a USGS-delineated sub basin, also presents the issue of having a very short measured reach within the sub basin and therefore very small changes in length, combined with changes due to where the river intersects the boundary, are amplified in the percent change calculations and disregarded in the analysis.

3.2. River Length and Sinuosity

The lengths of the river reaches were determined by calculating the geometry in the attribute table within ArcMap. Sinuosity, i.e. the ratio of the channel length to the valley length between two points on the river (Julien, 2018), was calculated using the straight line distance through each HUC12 as the "valley lengths" to spatially visualize sinuosity.

The drainage area was determined based on the USGS Watershed Boundary Dataset (WBD). WBD is a comprehensive hydrologic dataset, consistent with the national criteria for delineation and resolutions, which was created to encourage consistency and accuracy in

comparing hydrologic data (USGS, 2013). The national dataset delineates hydrologic unit codes (HUC) at varying scales, named for the number of digits assigned to the unit with HUC2 being the largest in area, and HUC12 being the smallest sub basin available for this area of interest. The Hydrologic Unit Code (HUC) 8 of the Amite River Basin measures 1,884 square miles, however, two additional HUC 10 units were included on the southern side of the basin to include the constructed Amite River Diversion Canal. Analysis of the DEM verified that it should be acceptable to include these basins, as they likely drain northeast into the Amite River since they are restricted from draining southwest into the Mississippi River by levees. However, the area is flat and marshy so water may flow east toward Lakes Maurepas and Pontchartrain rather than north to the Amite River Diversion Canal. The HUC 12 units are used in the study to divide the river into smaller, standardized units to measure changes in lengths and sinuosity throughout the basin for the four time periods.

3.3. River Characteristics

To prepare historical centerlines as input to the HEC-RAS Model, discussed in the next chapter, ArcMap was utilized to create the necessary shapefiles. First, the digitized centerlines for each time period were merged and cut to match the river segments needed in the model – Amite River above the confluence, Comite River above Pretty Creek, and Comite River above the confluence. Next, the banklines were merged and cut for the same segments used within the model. Then, simplified flow paths were created using the copy parallel tool in ArcMap, in a methodology described in the modeling chapter. Since the goal of this thesis research was to investigate the impacts length and sinuosity have on flood routing, and not to recreate historic conditions, the historical centerlines were used as realistic changes in length and sinuosity, but aggradation and

degradation along the channels were not accounted for and the cross section bathymetry was not changed.

CHAPTER 4. MODELING METHODS

4.1. Model Details

A calibrated and validated HEC-RAS coupled 1D/2D model of the Amite River Basin (Dewberry Engineers Inc., 2019) was used to simulate the flow and stage hydrographs at various cross sections along the Amite and Comite Rivers using the historical planform geometries. HEC-RAS version 5.0.6 was used to create and modify the model for this study. The United States Army Corps of Engineers' Hydrologic Engineering Center's River Analysis System (HEC-RAS) allows the user to perform one-dimensional steady flow, one and two-dimensional unsteady flow calculations, sediment transport/mobile bed computations, and water temperature/water quality modeling (hec.usace.army.mil/software/hec-ras/). The HEC-RAS 2D modeling capability uses a finite-volume solutions scheme and allows use of structured or unstructured mesh. A depth-average velocity is solved at each cell face of the mesh. This study will focus on the 1D portion of the model so more detail on the 1D capabilities will be described. The 1D capability utilizes a finite-difference solutions scheme. For 1D steady flow, water surface profiles are computed from one cross section to the next by solving the energy equations iteratively with the standard step method. The energy equation is written as:

$$Z_2 + Y_2 + \frac{a_2 V_2^2}{2g} = Z_1 + Y_1 + \frac{a_1 V_1^2}{2g} + h_e \quad (4\text{-}1)$$

where Z_1, Z_2 are elevations of the main channel invert, Y_1, Y_2 are depths of water at the cross sections, V_1, V_2 are average velocities, a_1, a_2 are velocity weighted coefficients, g is gravitational acceleration, and h_e is the energy head loss. Conveyance is calculated within each subdivision, the channel and two overbank areas, using the following form of the Manning's equation (for English units):

$$Q = KS_f^{1/2} \quad (4\text{-}2)$$

$$K = \frac{1.486}{n} AR^{2/3} \tag{4-3}$$

where Q is the flow, K is the conveyance for the subdivision, n is the Manning's roughness coefficient for the subdivisions, A is the flow area for the subdivision, R is the hydraulic radius for the subdivision (area divided by wetted perimeter), and S_f is the slope of the energy gradeline. Friction loss is determined in HEC-RAS by calculating the product of the friction slope and the discharge-weighted reach length, with the friction slope being calculated by Manning's equation (4-2) and the discharge-weighted reach length being calculated by the following equation:

$$L = \frac{L_{lob}\bar{Q}_{lob} + L_{ch}\bar{Q}_{ch} + L_{rob}\bar{Q}_{rob}}{\bar{Q}_{lob} + \bar{Q}_{ch} + \bar{Q}_{rob}} \tag{4-4}$$

where L_{lob}, L_{ch}, L_{rob} are the cross section reach length specified for flow in the left overbank, main channel, and right overbank, respectively and $\bar{Q}_{lob}, \bar{Q}_{ch}, \bar{Q}_{rob}$ are the arithmetic average of the flows between cross sections for the left overbank, main channel, and right overbank, respectively.

The 1D unsteady flow hydrodynamics are governed by the principles of conservation of mass (continuity) and momentum. The continuity equation can be written as follows:

$$\frac{\partial A}{\partial t} + \frac{\partial S}{\partial t} + \frac{\partial Q}{\partial x} - q_1 = 0 \tag{4-5}$$

where A is the cross-sectional area, t is time, S is the storage from the non-conveying portions of the cross section, Q is the flow, x is the distance along the channel, and q_1 is the lateral inflow per unit distance. Then the above continuity equation can be written for the channel and floodplain as follows:

$$\frac{\partial Q_c}{\partial x_c} + \frac{\partial A_c}{\partial t} = q_f \tag{4-6}$$

$$\frac{\partial Q_f}{\partial x_f} + \frac{\partial A_f}{\partial t} + \frac{\partial S}{\partial t} = q_c + q_l \tag{4-7}$$

where the subscripts c and f signify the channel and floodplain, respectively and q_l is the lateral inflow per unit length of floodplain and q_c and q_f are exchanges of water between the channel and floodplain. Within the HEC-RAS unsteady flow engine, the left and right overbanks are combined into a single flow compartment denoted as floodplain. The reach length for the floodplain is computed by calculating the arithmetic average of the left and right overbank reach lengths as follows:

$$L_F = \frac{(L_L + L_R)}{2} \tag{4-8}$$

where L_F, L_L, L_R are the reach lengths of the floodplain, left overbank, and right overbank, respectively. The continuity equations are approximated using implicit differences and solved. The momentum equation for a single channel is as follows:

$$\frac{\partial Q}{\partial t} + \frac{\partial (VQ)}{\partial x} + gA\left(\frac{\partial z}{\partial x} + S_f\right) = 0 \tag{4-9}$$

where Q is flow, t is time, V is average velocity, g is acceleration due to gravity, and S_f is friction slope. Again, the equation can be written for the channel and floodplain as follows:

$$\frac{\partial Q_c}{\partial t} + \frac{\partial (V_c Q_c)}{\partial x_c} + gA_c\left(\frac{\partial z}{\partial x_c} + S_{fc}\right) = M_f \tag{4-10}$$

$$\frac{\partial Q_f}{\partial t} + \frac{\partial (V_f Q_f)}{\partial x_f} + gA_f\left(\frac{\partial z}{\partial x_f} + S_{ff}\right) = M_c \tag{4-11}$$

where M_c and M_f are the momentum fluxes per unit distance exchanged between the channel and floodplain, respectively. Again, the above equations are approximated using implicit differences and solved (Brunner, 2016).

The specific model used in this study is the Amite River Basin Numerical Model (ARBNM), developed by the private consultant Dewberry with funding by the Louisiana Department of Transportation (LADOTD). The ARBNM is a basin-wide (approximately the HUC8 scale) model built with a suite of HEC software. The model's purpose is to provide planners

and engineers with a model representing the basin's current hydrologic and hydraulic condition. It was built with a tiered modeling approach using both 1D and 2D hydraulic approaches to add detail where needed to areas of greater flood risk or increased complexity (Dewberry Engineers Inc., 2019).

4.2. Sensitivity Analyses

Several sensitivity analyses were conducted before modifying the model to verify the methodology that was used and has been previously stated. Specifically, analyses were conducted to confirm the decisions to keep the cross section geometry constant for the various geometry runs, and to alter the reach lengths at each cross section to capture the change in length and sinuosity for each time period. First, how the shape of a cross section impacts the water surface elevation was tested, with the cross section area, top width, flow, slope, and Manning's roughness values held constant. A single reach, 1D steady-state model was built and run in HEC-RAS using a hypothetical, 14,000-ft long reach. Rectangular, trapezoidal, parabolic, triangular, and asymmetric triangular cross sections were tested, all with the same cross section area and top width. The model was run with normal depth downstream boundary condition, assuming subcritical flow, with three flows – 1000 cfs, 3000 cfs, and 6000 cfs, with the latter being the "bankfull discharge." The results showed that the water surface elevations varied more with lower flows than with the bankfull flow because the shapes differed the most at the channel bottom and had varying channel bed elevations, but once the channel was full, they all had the same area available. The triangular and asymmetric triangular cross section geometries showed the lowest water surface elevations because given the same area but varying shape, these cross sections were the deepest. The converse is true for the rectangular and trapezoidal cross section geometries, these were the shallowest and yielded the highest water surface elevations.

Given the over-simplified and unrealistic shape of the channels from the first analysis, a second sensitivity analysis was conducted using sample cross sections from the study area. One was taken from a bend (asymmetric shape) and one was taken from an inflection point (trapezoidal-type shape). In an attempt to keep the area and depth consistent, the asymmetric cross section resulted in a slightly smaller cross section area than the trapezoidal cross section. All other parameters were held constant and simulated at three flows, 1000 cfs, 3000 cfs, and 6000 cfs, assuming subcritical flow. The results showed lower water surface elevations for the trapezoidal channel, with a larger cross section area. This further verified the importance of keeping the cross section area constant and changing the depth accordingly. In the case of a cross section in a bend versus at an inflection point, the bend will be deeper due to the asymmetric shape and scour forces imposed by helical flow (Julien, 2018).

The impact of changing the "downstream reach lengths" within the HEC-RAS 1D cross section editor, without changing the terrain, was also investigated. This was investigated to decide if the historical length conditions were properly captured by modifying the lengths rather than altering the exact path the river follows in the terrain. An analysis was performed testing 1) a meandering reach with long, meandering reach lengths, 2) the same reach, but with a straightened centerline and therefore with shorter reach lengths, and 3) the meandering reach centerline, but with the shorter reach lengths input into RAS manually. The meandering reach was taken from a short section in the upper portion of the Amite River. HEC-RAS determines friction losses using the reach lengths, but these are typically calculated within RAS Mapper using georeferenced flow paths for the centerline and banks. The objective was to test if RAS would only consider the reach lengths in the loss calculations, or if other factors would impact the calculations. The cross section shapes and areas were held constant, as were the roughness values and the slope. The model was

run assuming subcritical flow at 1000, 3000 and 6000 cfs. The results showed case 2 and case 3, those with the same reach lengths but differing centerlines, were identical. It was determined that when using HEC-RAS 1D, the reach lengths are the only factor that will need to be edited to adequately model the intended friction losses due to longer and more sinuous river reaches.

The question also arose on how to determine flow paths for the historical cases. A test case of using these simplified flow paths was run in the model for the current conditions. One case used the flow paths that were initially delineated from the terrain and included in the model. The other case used flow paths that were created parallel to the river centerlines as a constant distance from the centerline. The runs were compared and no major differences were noted and therefore the simplified flow path methodology was adopted.

4.3. Model Modifications

The centerlines and banklines digitized from the historical USGS topographic maps were input into RAS Mapper, the GIS platform housed in the RAS software. Then, the overbank flow paths were added. The flow paths were created in ArcMap by using the editor tool to "copy parallel" the banklines at a uniform distance from the centerline that was estimated from the current conditions within the model. The existing cross sections from the ARBNM were employed to minimize errors at the 1D/2D connections and to keep the points of reference consistent when running the different historical centerlines. All of the model edits were completed within the 1D portion of the model, as Dewberry designed the model with wide cross sections to account for the possibility of incorporating historical meanders back into the river with relative ease. Utilizing the same cross sections for all time periods provides constant points in space where to compare changes in flow and stage of the river, although the lengths of river between the cross sections is changing. Once the river, banklines, and flow paths were added, RAS Mapper was then used to

compute the downstream reach lengths, taken from the intersection of the flow paths with the cross sections (Figure 5).

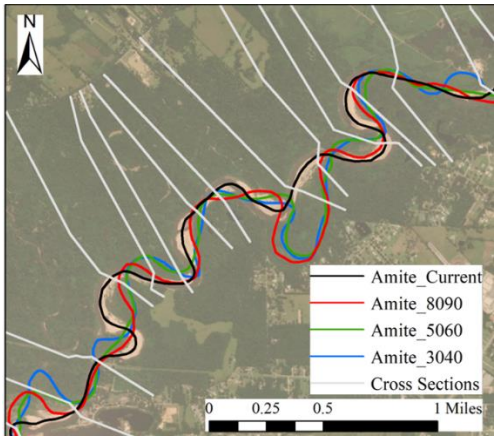

Figure 5. Example reach showing the historical centerlines and the model cross sections where the reach lengths for each centerline were calculated.

This step often introduced errors within the geometry. The best method to reduce this error was to use RAS Mapper to compute the reach lengths in one geometry file, and then copy these reach lengths from the reach lengths table in the geometry editor window of HEC-RAS to paste into the geometry layer that will be used to run the model. The cross section area of each cross section was kept consistent because the bankfull runoff is assumed to remain constant. Additionally, since 1D HEC-RAS uses the reach lengths to determine the friction losses between cross sections and the cross section area was held constant, the only modification determined necessary to reflect the historical length and sinuosity conditions was altering the reach lengths. Therefore, the cross section geometry was not altered. The study's objective is to test the impact of the changes in river length and sinuosity on water surface elevation and flow, and any channel aggradation or degradation is ignored. The Manning's roughness values are also assumed to remain the same in the historical conditions, which is a limitation since the disturbances along the river have likely impacted the roughness values. For instance, dredging of the river would result in lower Manning's values inside the channels for the current case and urbanization would result in added concrete,

yielding lower Manning's roughness values as well. The bathymetry used was collected by the USACE and Forte and Tablada in 2017 using GPS and conventional surveying, and bathymetric surveying methods when excessive water depths were encountered (Dewberry Engineers Inc., 2019).

4.4. Rainfall Events

Four rainfall events were run for the four geometry scenarios. The chosen four events were the historical flows that were used as calibration events in the model and had a range of magnitudes that varying spatially across the basin (Figure 6). The rainfall was input as gridded rainfall data into HEC-HMS, the hydrologic HEC software, and the discharge outputs were then input to the HEC-RAS portion of the ARBNM. The distribution of the rainfall events vary by storm which is expected to impact which rainfall events elicit larger or smaller responses, depending on if the majority of rain fell upstream or downstream of the areas with the greatest planform geometry changes. The March 2016 event had more rain over the eastern portion of the basin, so there may be more impacts seen on the routing along the Amite River. Also, there was a concentration of rain downstream of the confluence so impacts due to backwater effects could be observed (Figure 6a). The majority of the rain for the August 2016 event fell upstream of the confluence and slightly more fell on the western side of the basin over the Comite River (Figure 6b). August 2017 showed about equal distribution of rain over the Amite and Comite rivers, slightly favoring the Amite, but much of the rain for this smaller event fell downstream of the confluence so large responses in the routing are not expected (Figure 6c). October 2017 also saw about equal distribution of rain over the Amite and Comite Rivers, this time slightly favoring the Comite River and with most of the rain falling higher in the basin and therefore hopefully eliciting a more noticeable response in the routing results (Figure 6d.)

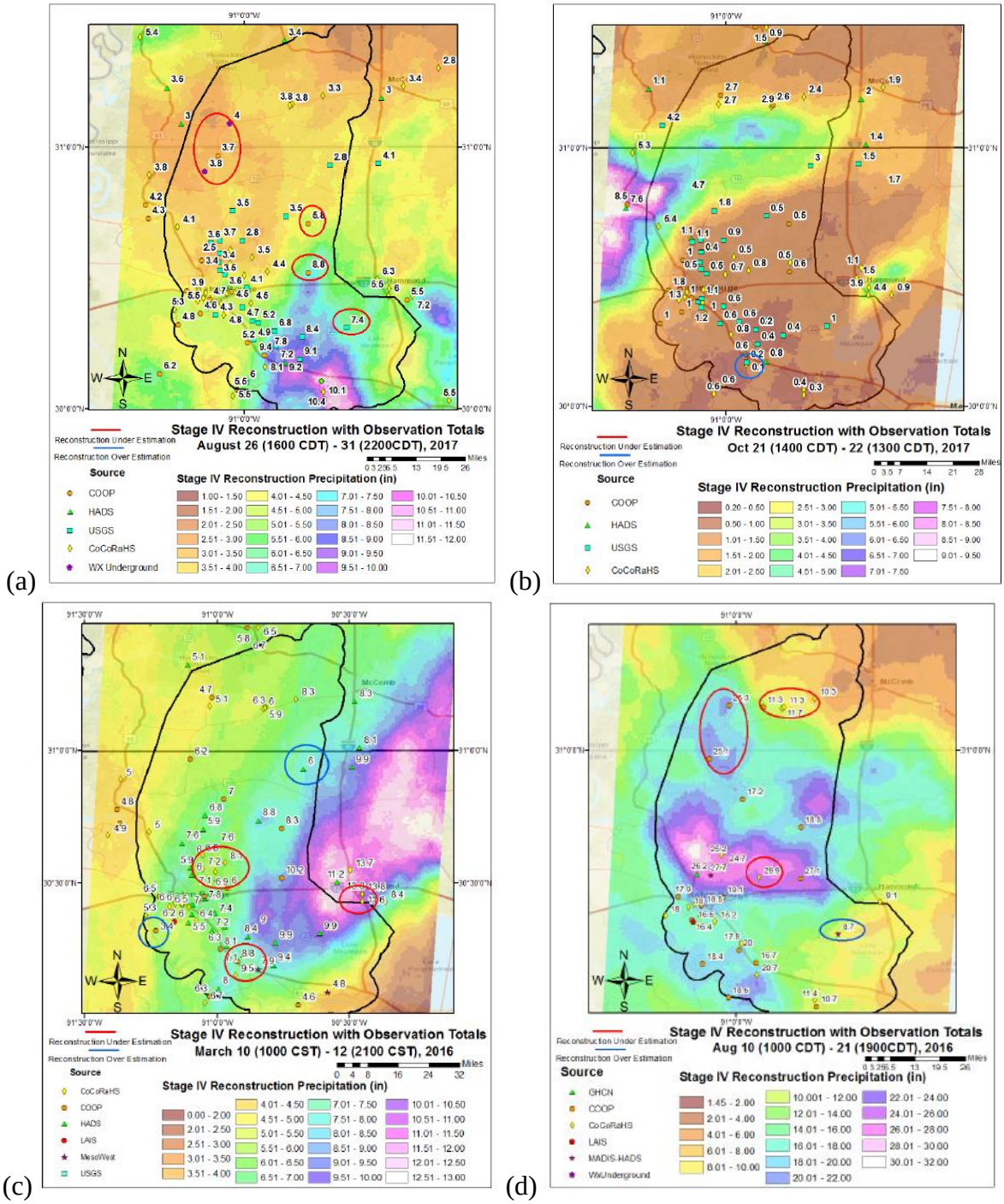

Figure 6. Rainfall distributions run in the ARBNM for the four events (a) August 2017, (b) October 2017, (c) March 2016, and (d) August 2016 (Dewberry Engineers Inc., 2019).

Table 2. Flow events and their corresponding return periods at the Darlington USGS gage, on the upper portion of the Amite River, the Denham Springs USGS gage, just downstream of the confluence of the Amite and Comite Rivers, and the Olive Branch USGS gage, on the upper portion of the Comite River. Gage locations are given in Figure 9.

Event	Peak Flow (cfs)	Return Period
Amite at Darlington		
August 2017	4,200	1 - year
October 2017	12,700	1.4 - year
March 2016	24,900	3 - year
August 2016	116,000	100 - year
Amite at Denham Springs		
August 2017	7,740	1 - year
October 2017	25,100	1.6 – year
March 2016	64,900	6 - year
August 2016	266,000	> 500 - year
Comite at Olive Branch		
August 2017	2,565	1 - year
October 2017	9,096	2.4 - year
March 2016	10,101	2.8 - year
August 2016	72,642	500 - year

CHAPTER 5. RESULTS

5.1. River Length and Sinuosity Calculations

Once the topographic maps were digitized, the length and sinuosity within each HUC12 unit were calculated and the basin and percent change in length and sinuosity for each HUC12 between each time period and overall was calculated and compared (Table 3, Figure 7, Figure 8). Both rivers exhibited an overall decrease in length and sinuosity: a 6% decrease on the Comite and an 8% decrease on the full Amite River. It should be noted that the majority of the decrease in length and sinuosity on the Amite River occurred upstream of the confluence with a 13% decrease overall, whereas downstream of the confluence only experienced a 1% decrease. Additionally, within the rivers, the changes are both spatially- and temporally-dependent. Most of the Comite decrease occurred between the 1930's and 1950's. Specifically, the Hurricane Creek HUC12 decreased in length by 21% in this time period, which is also the time period East Baton Rouge Parish, which includes the Hurricane Creek HUC12, showed the greatest increase in population. This also corresponds spatially and temporally with the enlargement and realignment projects conducted along this portion of the Comite River to increase conveyance of water down the river and allow more area to be suitable for development to accommodate the growing population (USACE, 1955). Most of the Amite decreases occurred between the 1950's and 1980's; Clear Creek, Pigeon Creek, and Kidds Creek decreased by 10, 15, and 8%, respectively. This coincides with the spatial center and temporal peak of sand and gravel mining in the Amite River Basin (Hood, Patrick, & Corcoran, 2007).

Table 3. Measured length, sinuosity, and percent change in length and sinuosity per each HUC12 of the main stems of the Amite and Comite Rivers. “Total Amite US” refers to upstream of the confluence with the Comite River and “Total Amite DS” refers to downstream of the confluence.

HUC12	Length (mi)					Sinuosity				Percent Change			
Comite	Valley Length	30/40	50/60	80/90	2017	1930/40	1950/60	1980/90	2017	1930/40-1950/60	1950/60-1980/90	1980/90-2017	Total
Richland Creek	3.6	7.0	6.2	6.0	6.3	1.93	1.69	1.66	1.73	-12%	-2%	4%	-11%
Pretty Creek	7.6	13.5	14.0	13.6	14.4	1.77	1.84	1.79	1.90	4%	-3%	6%	7%
Knighton Bayou	13.3	21.6	21.1	21.0	19.5	1.62	1.58	1.57	1.47	-2%	-1%	-7%	-10%
Blackwater Bayou	9.8	12.3	12.7	12.1	12.3	1.26	1.30	1.23	1.26	3%	-5%	2%	0%
Hurricane Creek	7.0	11.9	9.4	9.6	9.8	1.70	1.34	1.37	1.41	-21%	2%	3%	-17%
Total Comite	**41.4**	**66.3**	**63.4**	**62.2**	**62.4**	**1.60**	**1.53**	**1.50**	**1.51**	**-4%**	**-2%**	**0%**	**-6%**
Amite													
Cars Creek	0.7	0.9	0.9	1.0	1.1	1.32	1.32	1.47	1.62	0%	12%	10%	23%
Clear Creek	10.7	18.2	17.8	15.9	15.0	1.71	1.67	1.49	1.41	-2%	-10%	-6%	-18%
Pigeon Creek	8.5	13.5	13.4	11.4	10.0	1.58	1.57	1.33	1.17	0%	-15%	-12%	-26%
Kidds Creek	12.3	19.0	18.1	16.8	16.1	1.54	1.48	1.36	1.31	-4%	-8%	-4%	-15%
Beaver Creek	8.8	14.0	13.5	14.0	14.5	1.59	1.54	1.60	1.65	-3%	4%	3%	4%
Total Amite US	**40.9**	**65.6**	**63.8**	**59.1**	**56.8**	**1.60**	**1.56**	**1.44**	**1.39**	**-3%**	**-7%**	**-4%**	**-13%**
Clay Cut Bayou	17.7	29.5	27.8	28.0	28.5	1.66	1.57	1.58	1.61	-6%	1%	2%	-3%
King George Bayou	8.6	14.2	14.3	14.3	14.7	1.66	1.67	1.67	1.72	1%	0%	3%	3%
Bayou Barbary	7.3	12.1	12.0	12.0	12.1	1.66	1.65	1.65	1.66	-1%	0%	1%	0%
Total Amite DS	**33.6**	**55.8**	**54.1**	**54.4**	**55.3**	**1.66**	**1.61**	**1.62**	**1.65**	**-3%**	**1%**	**2%**	**-1%**
Total Amite	**74.5**	**121.4**	**117.9**	**113.5**	**112.1**	**1.63**	**1.58**	**1.52**	**1.50**	**-3%**	**-4%**	**-1%**	**-8%**

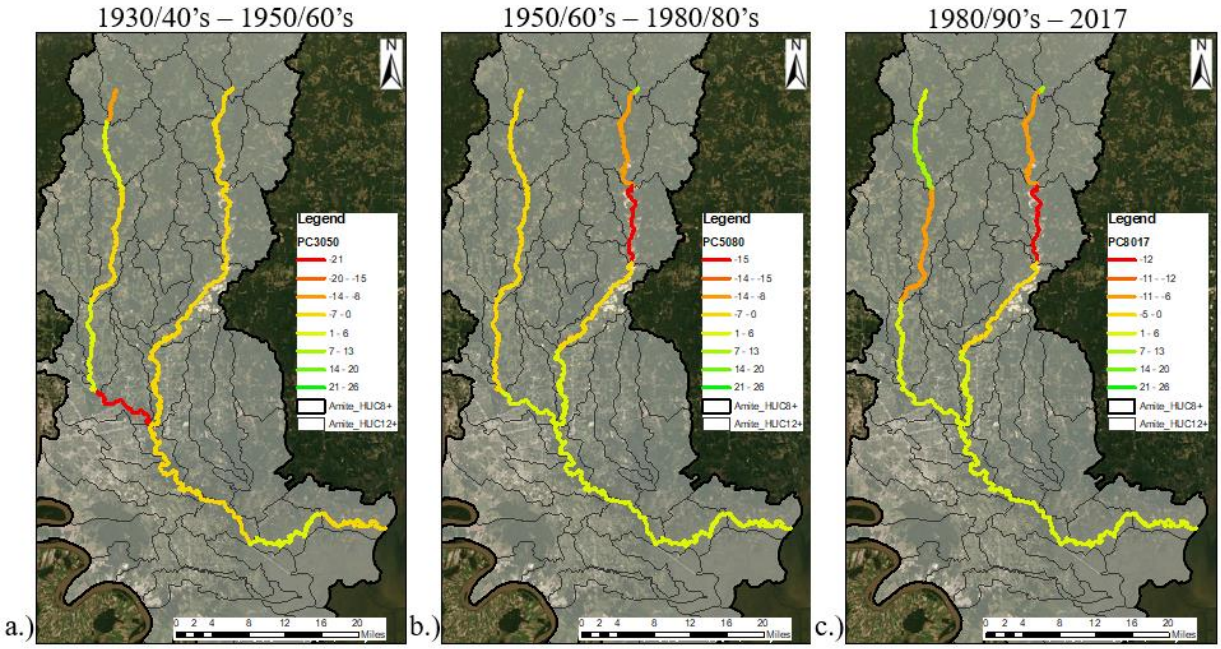

Figure 7. Changes in length and sinuosity by HUC12 by time period.

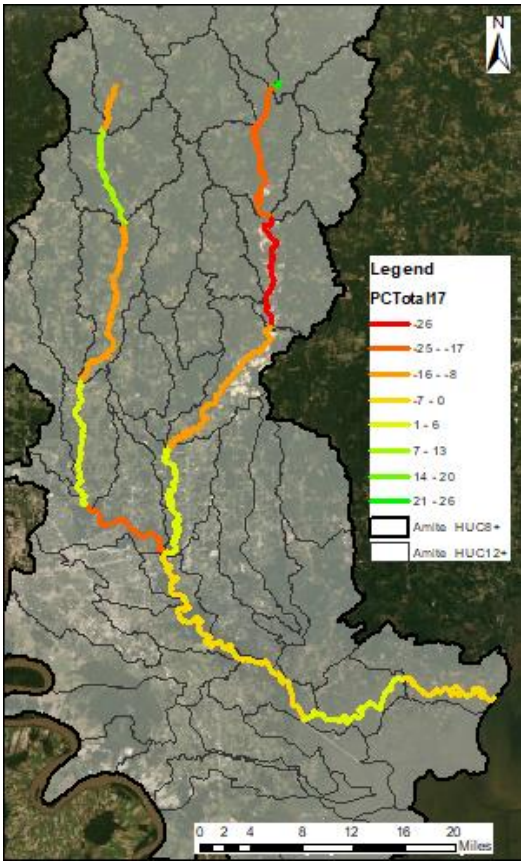

Figure 8. Map of HUC12 units corresponding the overall percent change in sinuosity (30/40s to present) presented in Table 3.

5.2. Modeling Results

The ARBNM was run for the four historical planform geometry scenarios, each for the four rainfall events, for a total of sixteen runs. Results are shown at five cross sections along the Amite and Comite Rivers (Figure 9). The first set of results presented in this section are for the two upstream-most cross sections on the Amite and Comite Rivers, respectively, that are used in the model. The upstream-most cross section on the Amite is cross section 624771.4 and on the Comite is cross section 342648.6. These numbers are the cross section names and are given based on the distance the cross section is upstream of the start of the particular river for the 2017 conditions, given in feet (Dewberry Engineers Inc., 2019). Here the numbers are used solely to name that certain cross section location in space. These first two cross sections are upstream of

any alteration made in the model and therefore the results should not reflect changes in length and sinuosity. The next set of results are for the Amite River cross section 296046.6, which is the downstream-most cross section on the Amite River above its confluence with the Comite River and therefore a representation of the cumulative impacts of the planform geometry change along the Amite River upstream of the confluence. Next, results are presented for the Comite River cross section 1188.23, which is likewise the downstream-most cross section on the Comite River above its confluence with the Amite River and therefore a representation of the cumulative impacts of the planform geometry change along the Comite River. Finally, results are shown for the Amite River cross section 295071.9, which is the cross section directly downstream the confluence and represents the effect of the coupled impacts along the Amite and Comite Rivers. The y-axes of all the hydrograph plots do vary between storms and sometimes cross sections. The y-axes on the flow hydrographs are consistent among plots for the same storm event so that the relative flow at that cross section can be noted, but they vary between storms since each event varies widely, ranging from 1- to greater than 500-yr return period flow events. The y-axes on the stage hydrographs vary due to the changes in elevation at different cross sections, but the amount the axis ranges is consistent among plots for the same events. Again, the ranges vary between the different storm events due to the varying magnitude of the events. All hydrograph plots have an x-axis that spans seven days so no horizontal distortion is present.

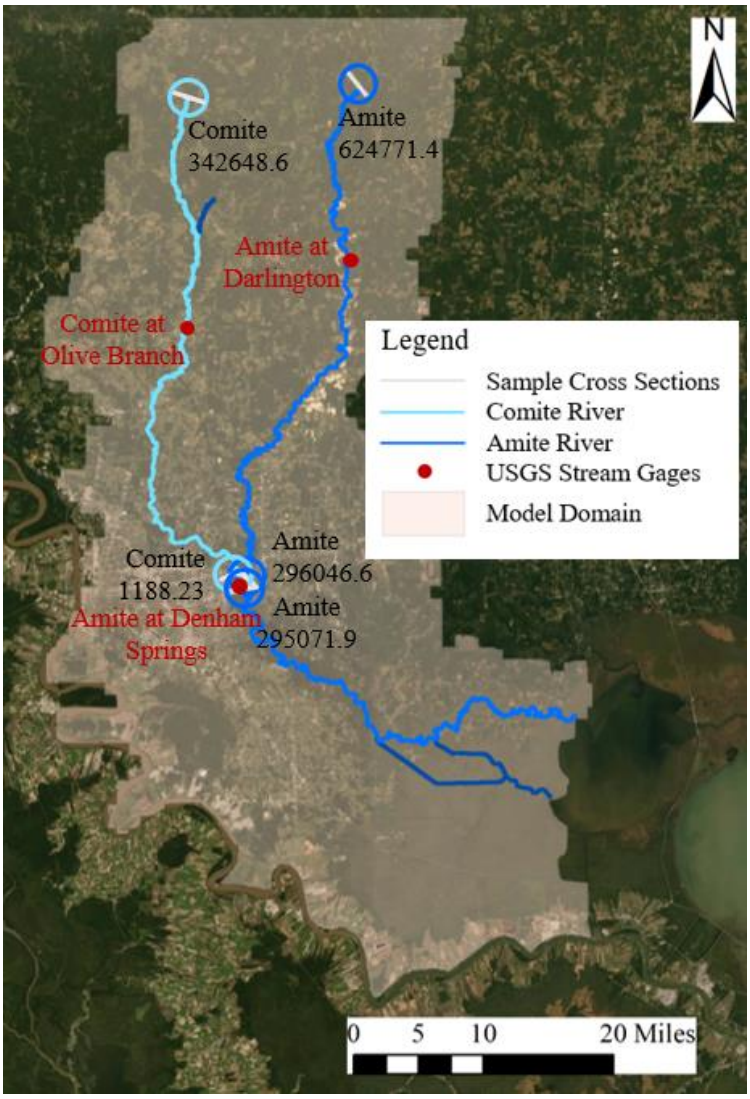

Figure 9. Locations of the sample cross sections on the Amite and Comite Rivers were results are shown and the gage locations where the flow return periods are calculated for each rainfall event (Table 2).

At the Amite River cross section 624771.4, the upstream-most cross section on the Amite within the model, the flow between the 4 historical planform geometry scenarios are identical for the four storm events (Figure 10). Since the cross section is above all portions of the river that changed in length and sinuosity over time, no change in flow is expected and this shows the same starting flow condition for all the historical planform geometry scenarios. The stages vary by less than 1.5 feet and less than 1% in all cases and the only variation is seen between the 1980/90s and current (Figure 11).

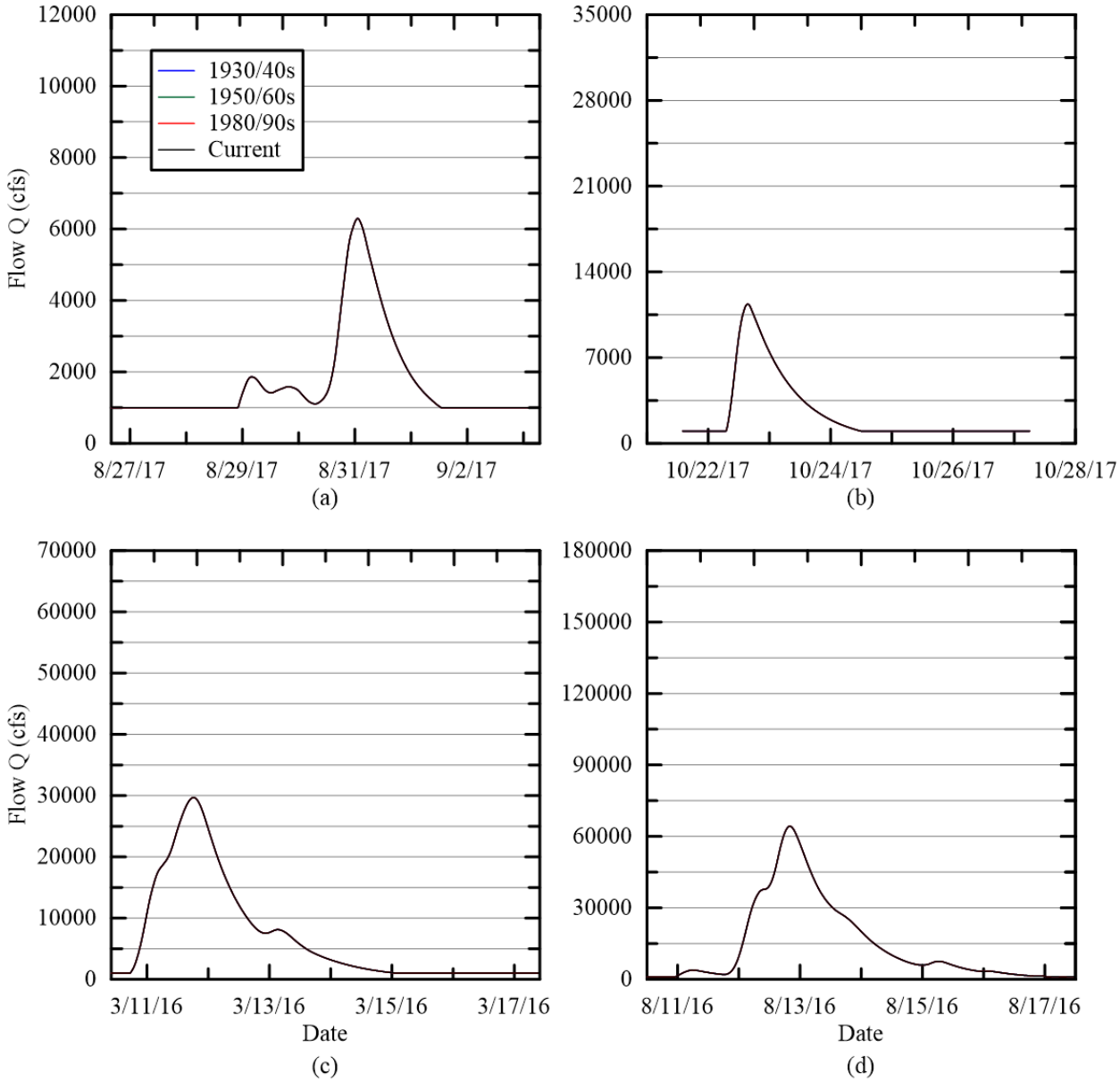

Figure 10. Flow hydrographs for Amite River 624771.4, the upstream-most cross section on the Amite River, for the four flow events (a.) August 2017, (b.) October 2017, (c.) March 2016, and (d.) August 2016.

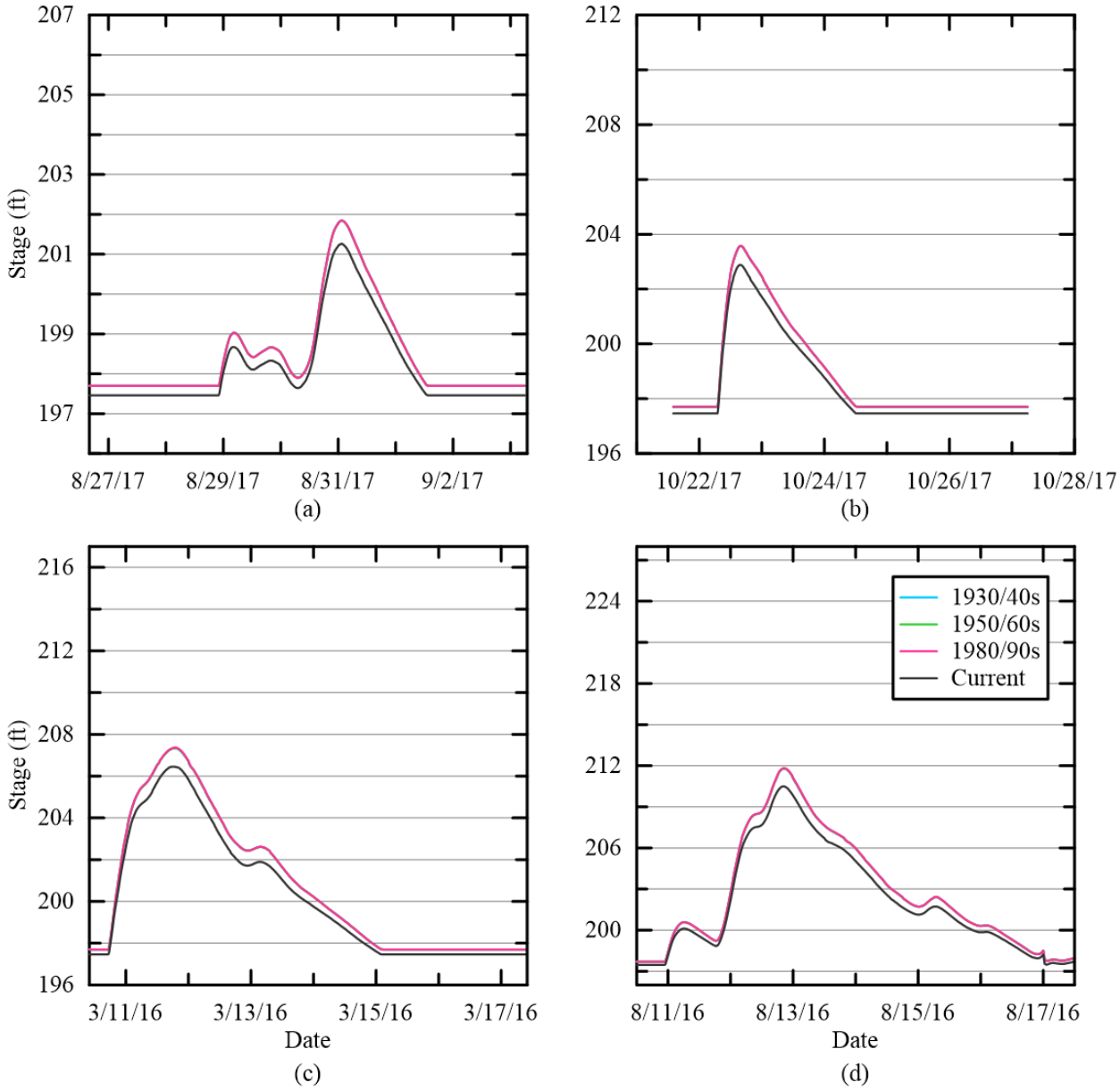

Figure 11. Stage hydrographs for Amite River 624771.4, the upstream-most cross section on the Amite River, for the four flow events (a.) August 2017, (b.) October 2017, (c.) March 2016, and (d.) August 2016.

Likewise, the Comite River cross section 342648.6, the upstream-most cross section on the Comite River within the model, shows identical flow for the four historical planform geometry scenarios for the four flow events (Figure 12). The stages vary slightly among the different historical planform geometry scenarios, but the differences are less than 1 feet and less than 0.5%

(Figure 13). This small to no change is what is expected at this cross section since it is upstream of the disturbances and the start of the model flow routing.

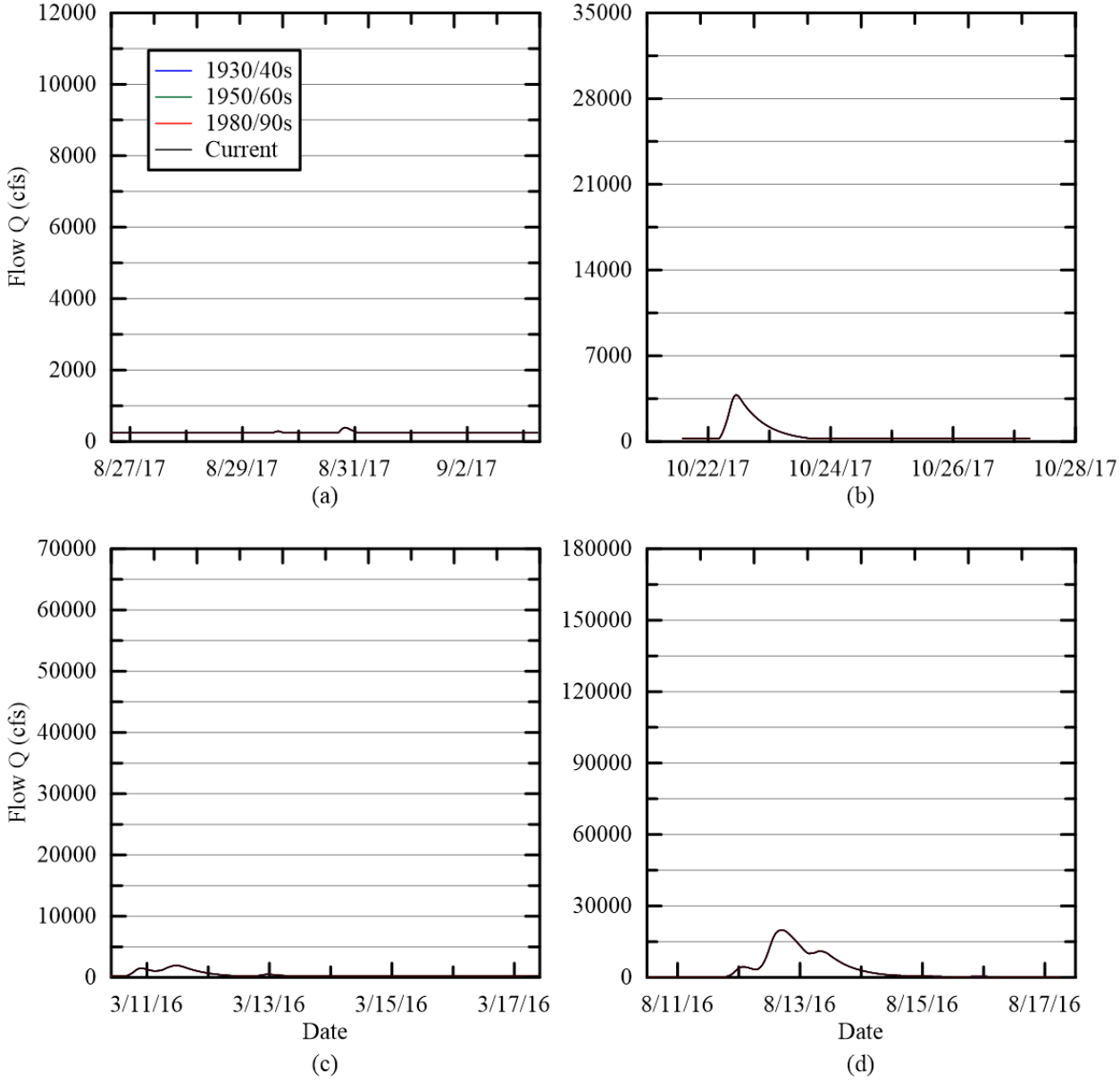

Figure 12. Flow hydrographs for Comite River 342648.6, the upstream-most cross section on the Comite River, for the four flow events (a.) August 2017, (b.) October 2017, (c.) March 2016, and (d.) August 2016.

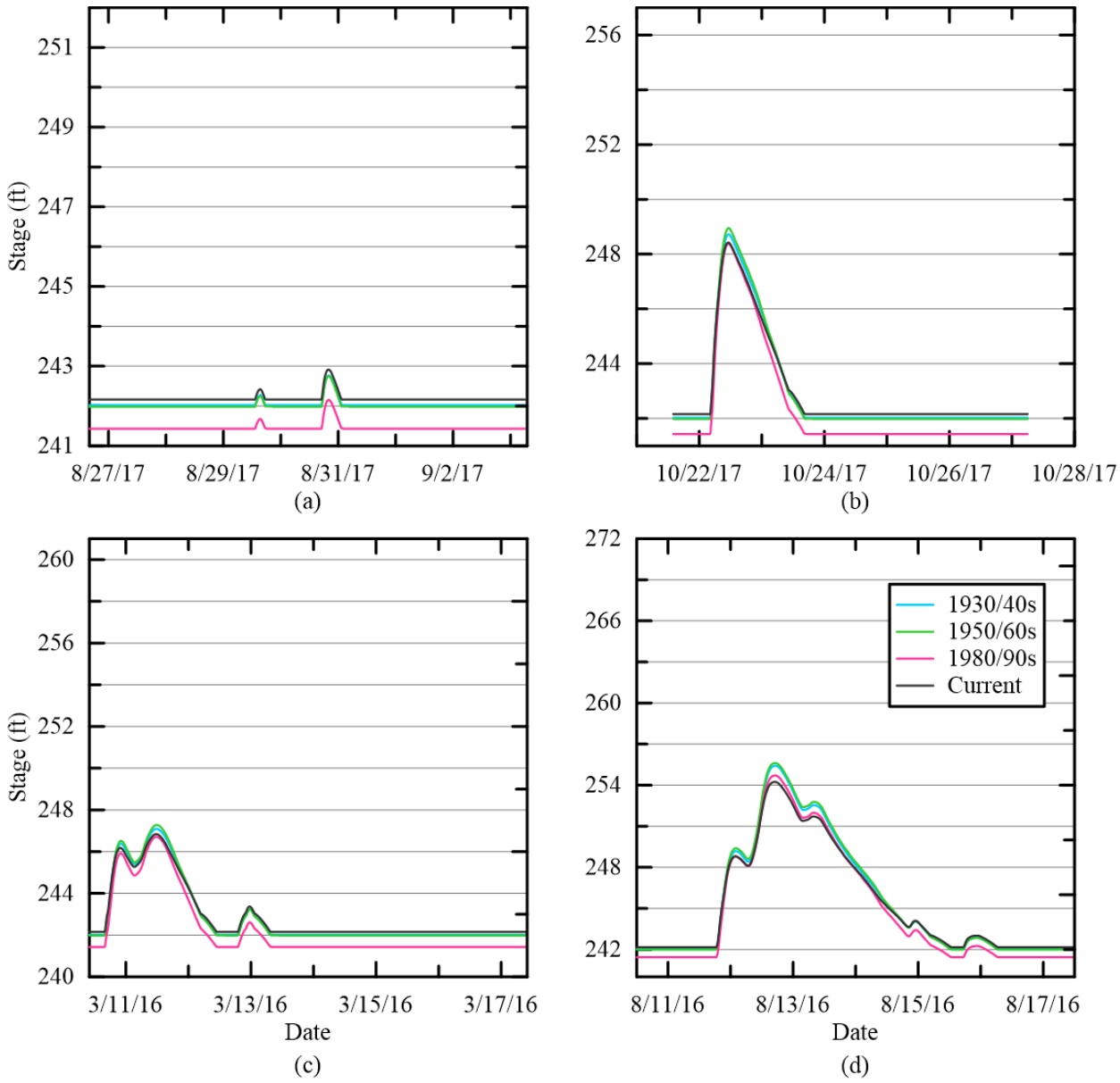

Figure 13. Stage hydrographs for Comite River 342648.6, the upstream-most cross section on the Comite River, for the four flow events (a.) August 2017, (b.) October 2017, (c.) March 2016, and (d.) August 2016.

The Amite River cross section 296046.6, just upstream of the confluence, shows overall decreases in peak magnitude and delay in peak arrival time for both stage and flow for the four events in the older, more sinuous geometries compared to the current conditions (Figure 14, Figure 15).The percent changes in peak flow magnitude were the most consistently noticeable for the August 2016 and March 2016 events which are the larger, out-of-bank events (Figure 16a).

The percent change in peak stage heights behaved in similar patterns to the flow, but the values were on average lower than those seen with flow and a greater relative response was seen for the October 2017 event, which is considered a bankfull discharge (Figure 16c). The difference in magnitude of the percent change in flow versus percent change in stage is likely because greater flows only results in small increases in stage, as seen with how a rating curve will flatten out at the higher flow values.

When viewing the results grouped into time period, and therefore reflections of changes between historical planform geometry scenarios, and comparing with the corresponding historical change in sinuosity, the changes in peak flow and stage follow the expected trend of increasing in peak magnitude as sinuosity in the river decreases for the March 2016 and August 2016 events. The exception is 8090-Current in which a smaller increase would be expected given the smaller change in sinuosity change (Figure 16b, Figure 16d). Overall, there are not clear relationships between an increase in peak with a decrease in sinuosity between each of the three time periods, but there is an overall decrease in sinuosity that corresponds to an overall increase in peak magnitude.

Most cases resulted in peak arrival times that were earlier for the current condition than they were for the older, more sinuous geometry scenarios (Table 4). The arrival time difference was calculated by subtracting the earlier time period from the more recent time periods, (e.g. current – 8090), so the negative arrival time differences mean the peak arrived earlier with the more recent planform geometry scenario, which is what would be expected if a river decreases in length and sinuosity. The peaks for both stage and flow at the Amite River upstream of the confluence arrived earlier for the current conditions compared to the earliest, 3040 (1930/40s) scenario for all four flow events. The only cases that resulted in later arrival times were a few

seen between 8090 and current. The greatest changes in arrival time resulted from August 2016 for the stage and October 2017 for the flow and the smallest change resulted from March 2016 for both stage and flow.

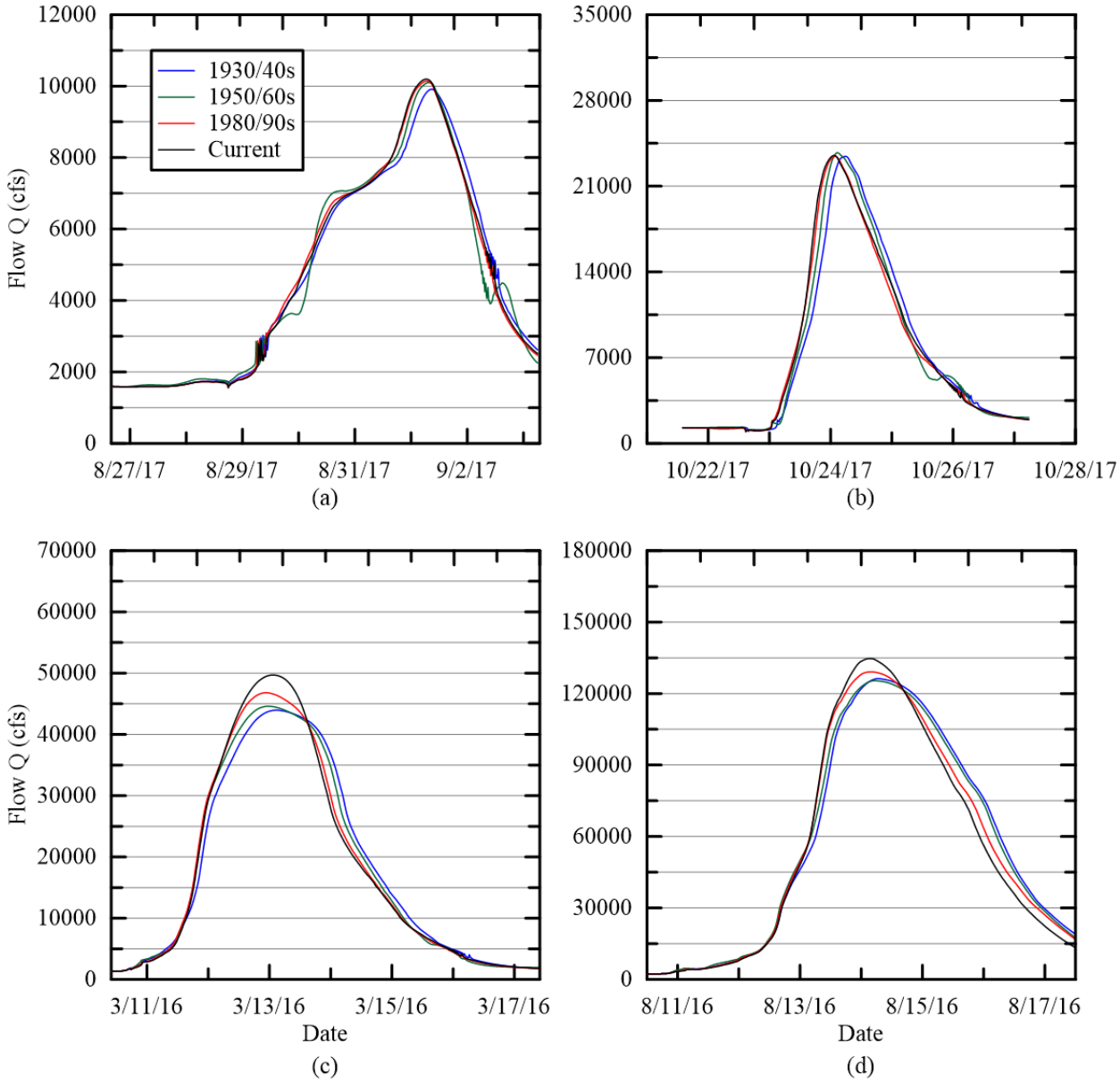

Figure 14. Flow hydrographs for Amite River 296046.6, the cross section directly upstream of the confluence for the four flow events (a.) August 2017, (b.) October 2017, (c.) March 2016, and (d.) August 2016.

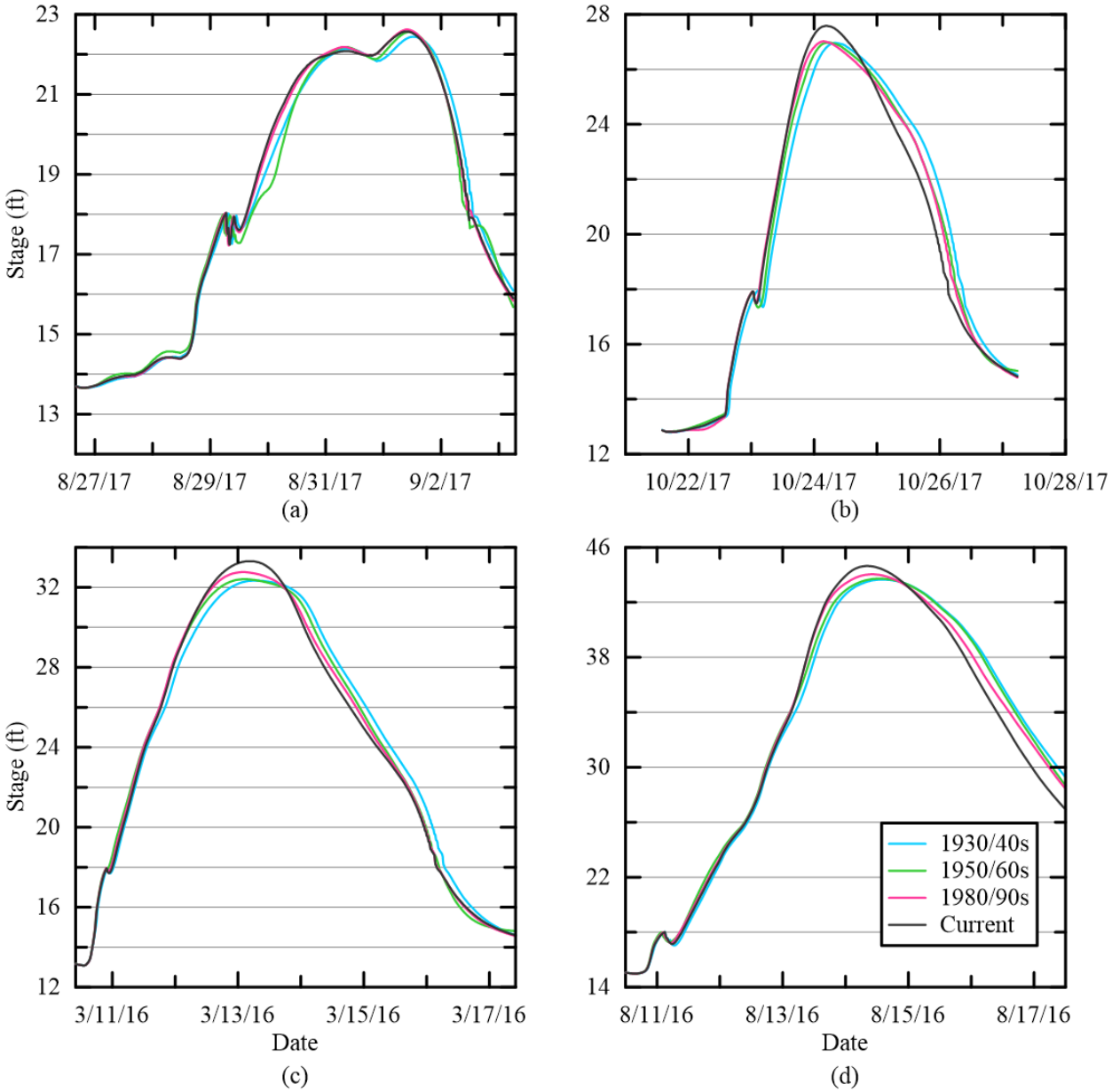

Figure 15. Stage hydrographs for Amite River 296046.6, the cross section directly upstream of the confluence for the four flow events (a.) August 2017, (b.) October 2017, (c.) March 2016, and (d.) August 2016.

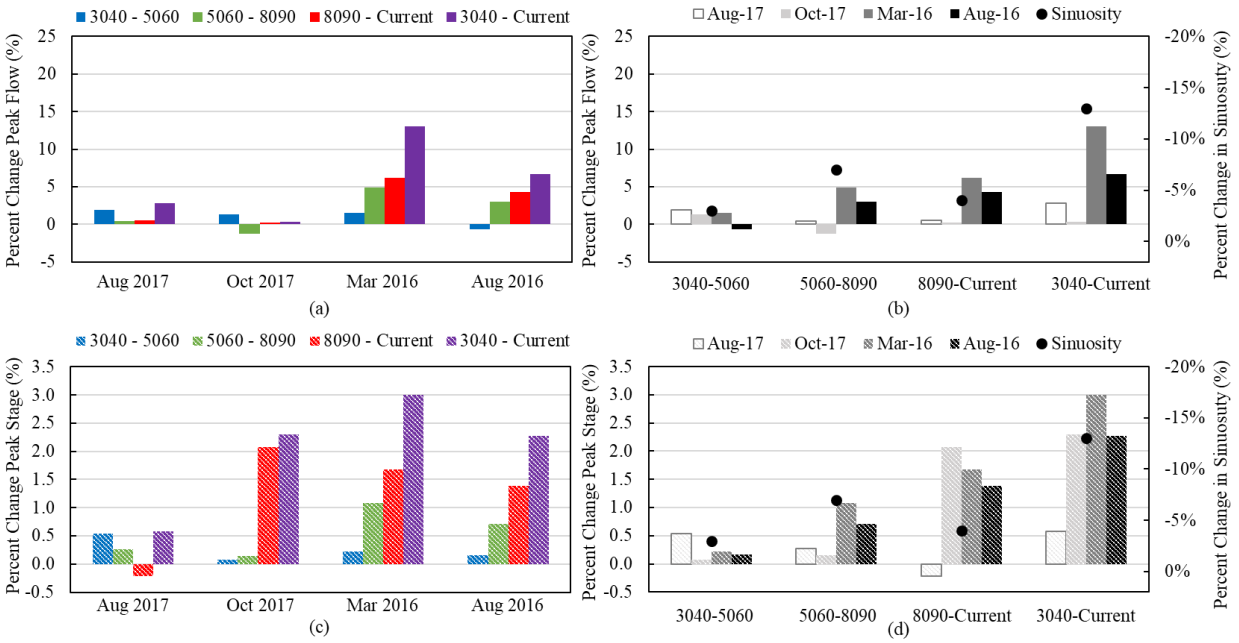

Figure 16. Percent change in (a.) flow, grouped by storm event, (b.) flow, grouped by differences between historical scenarios with the corresponding change in length/sinuosity, (c.) stage, grouped by storm events, (b.) stage, grouped by differences between historical scenarios with the corresponding change in length/sinuosity and Amite River cross section 296046.6.

Table 4. Values for the difference in peak magnitude, percent change in peak magnitudes, and difference in arrival time for stage and flow for the four rainfall events between the geometry scenarios at Amite River cross section 296046.6.

Event	Historic Geometry Scenario	Peak Difference (cfs)	Percent Change (%)	Arrival time difference (hr)	Peak Differnce (ft)	Percent Change (%)	Arrival time difference (hr)
August 2017	3040 - 5060	188.86	1.91	-1.2	0.12	0.53	-1.7
	5060 - 8090	41.85	0.41	-1.0	0.06	0.27	-0.8
	8090 - Current	52.62	0.52	0.0	-0.05	-0.22	-0.5
	3040 - Current	283.33	2.86	-2.2	0.13	0.58	-3.0
October 2017	3040 - 5060	305.24	1.30	-3.2	0.02	0.07	-2.0
	5060 - 8090	-293.47	-1.24	-0.8	0.04	0.15	-2.2
	8090 - Current	56.93	0.24	-0.5	0.56	2.07	0.8
	3040 - Current	68.7	0.29	-4.5	0.62	2.30	-3.3
March 2016	3040 - 5060	649.02	1.48	-3.2	0.07	0.22	-3.8
	5060 - 8090	2203.15	4.94	-1.0	0.35	1.08	-0.5
	8090 - Current	2891.62	6.18	2.8	0.55	1.68	2.3
	3040 - Current	5743.79	13.07	-1.3	0.97	3.00	-2.0
August 2016	3040 - 5060	-881.6	-0.70	-1.5	0.07	0.16	-1.0
	5060 - 8090	3718.4	2.97	-1.5	0.31	0.71	-2.5
	8090 - Current	5595.3	4.33	0.0	0.61	1.39	-1.5
	3040 - Current	8432.1	6.68	-3.0	0.99	2.27	-5.0

The Comite River cross section 1188.23 shows an overall decrease in peak flow magnitude with slight delays in peak arrival time for older, more sinuous geometries compared to current (Figure 17). The peak stage magnitudes are also lower, the hydrographs are wider, and the arrival time is slightly delayed for the older, more sinuous geometry scenarios (Figure 18). A particularly interesting case is the October 2017 event. The current conditions hydrograph shows one, large peak whereas the historical cases show two, smaller peaks resulting in shorter and wider hydrograph shapes (Figure 17b). This is likely due to spatially variable changes in sinuosity along the Comite causing the flow to be delayed in certain areas, allowing the temporally-varied rainfall to appear in two distinct peaks. However, the shift from one large peak to two smaller peaks for the October 2017 event is not in the stage hydrographs (Figure 18b).

The percent change values for flow are highest for the Comite cross section, just upstream of the confluence compared to the percent change values on the Amite upstream and downstream of the confluence. This could be due to the cumulative impacts of changes in river length along the Comite River, or due to the spatial distribution of the rainfall favoring the Comite and amplifying the response seen (Figure 19a). October 2017 showed the greatest percent change in flow, likely due to the shift in the hydrograph shape, with March 2016 and then August 2016 following in magnitude of change for flow (Figure 19a). The percent change in stage was most apparent for the March 2016 event, with October 2017 and August 2016 also showing significant overall percent changes (Figure 19c). August 2017 showed the smallest percent change in peak magnitude for both flow and stage, with nearly no change in stage. Again, like on the Amite, the percent change values seen for flow are much higher than those seen for stage.

When comparing percent change in peak magnitude with time and the corresponding change in sinuosity, again the relationships are not clear for the intermediate time periods. The

percent change in peak flow initially decreases with a decrease in change in sinuosity for the 3040-5060 and 5060-8090 cases, which is what is expected, but then a smaller change in sinuosity corresponds with a greater change in peak flow for the 8090-Current case (Figure 19b), similar to what is seen on the Amite upstream of the confluence. Percent change in peak stage appears to have the opposite relationship with percent change in sinuosity as expected – at this cross section greater decreases in sinuosity correspond to smaller changes in peak flow magnitude (Figure 19d). Both flow and stage show the greatest decreases in sinuosity and increased in peak magnitude for the cumulative time period.

The peak flows arrival times were rather erratic at this cross section, with earlier peaks for the current for the two larger events March 2016 and August 2016 and later peaks for current for the two smaller events August 2017 and October 2017 (Table 5). The peak stages arrived earlier overall for the current scenarios compared to the earlier, 3040 scenarios, with the greatest impacts seen for the August 2016, the largest event.

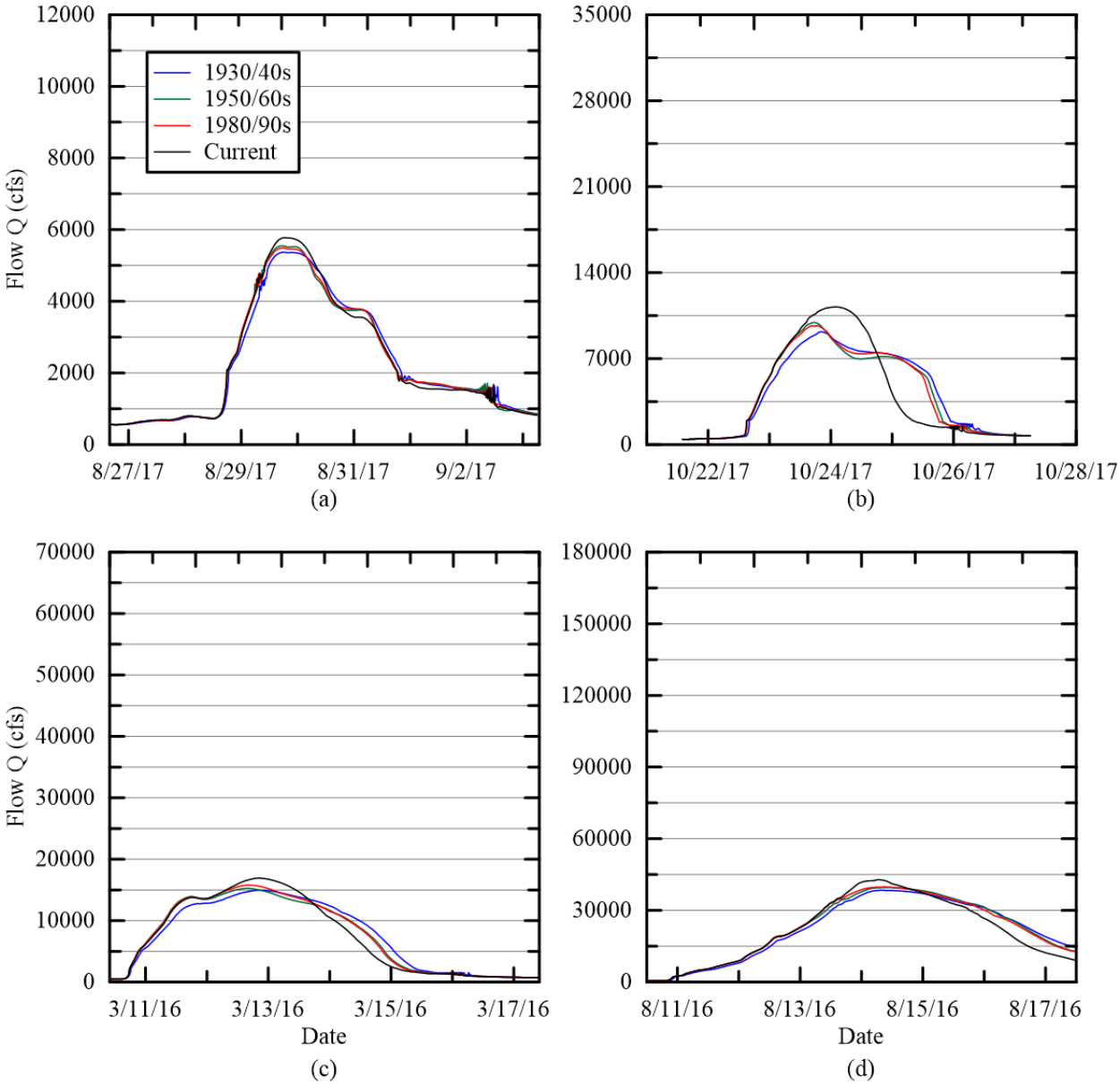

Figure 17. Flow hydrographs for Comite River 1188.23, the cross section directly upstream of the confluence for the four flow events (a.) August 2017, (b.) October 2017, (c.) March 2016, and (d.) August 2016.

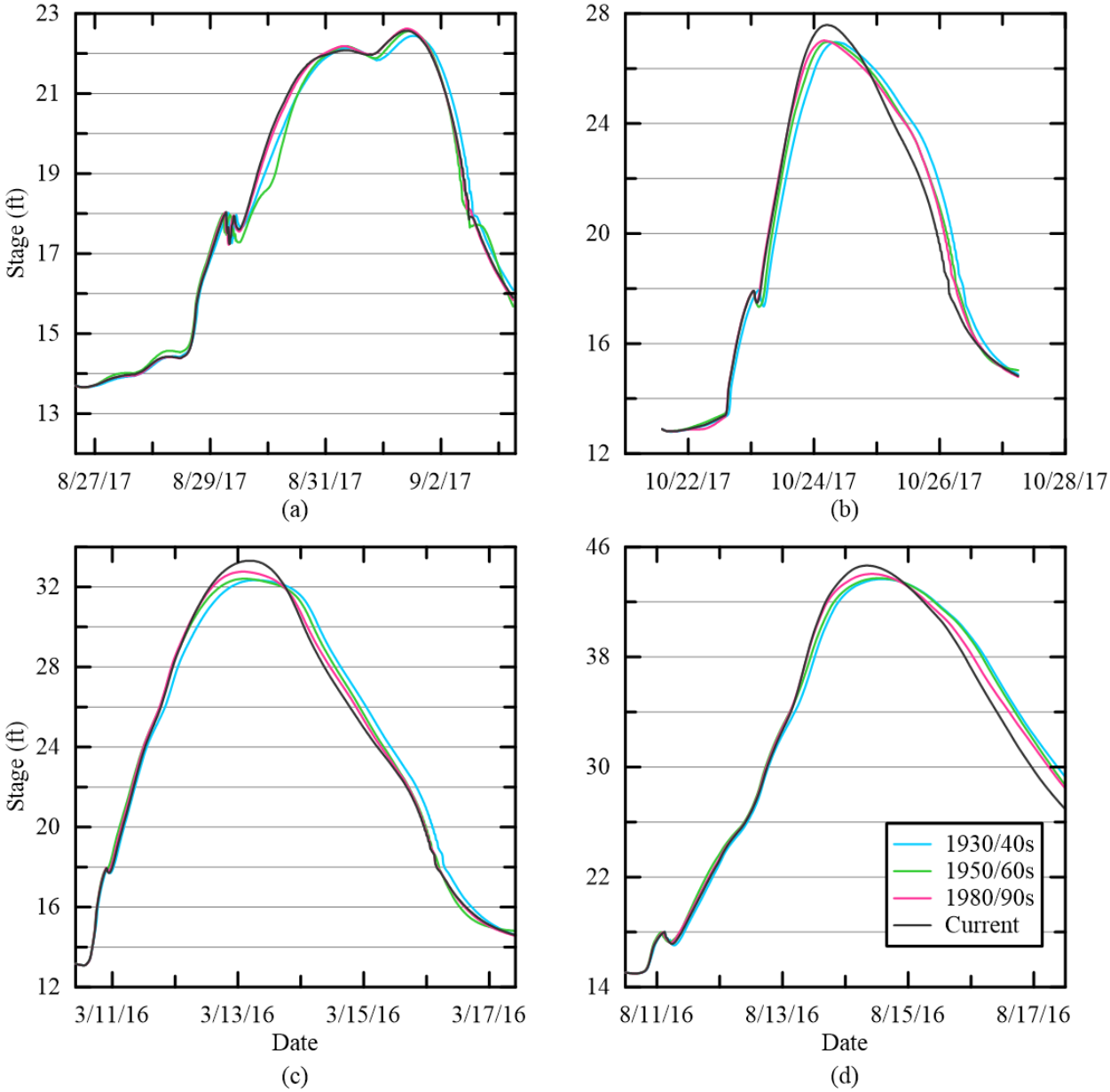

Figure 18. Stage hydrographs for Comite River 1188.23, the cross section directly upstream of the confluence for the four flow events (a.) August 2017, (b.) October 2017, (c.) March 2016, and (d.) August 2016.

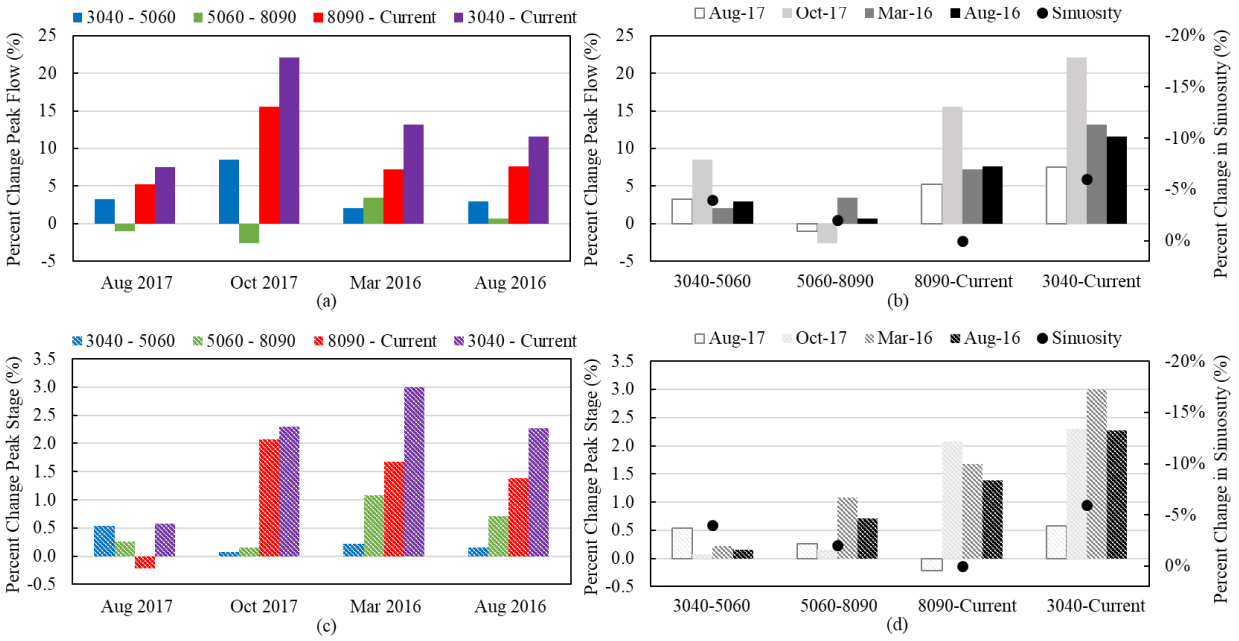

Figure 19. Percent change in (a.) flow, grouped into storm events, (b.) flow, grouped into differences between geometry scenarios with the corresponding change in length/sinuosity, (c.) stage, grouped into storm events, (b.) stage, grouped into differences between historical scenarios with the corresponding change in length/sinuosity for Comite River 1188.23.

Table 5. Values for the difference in peak magnitude, percent change in peak magnitudes, and difference in arrival time for stage and flow for the four rainfall events between the geometry scenarios at Comite River cross section 1188.23.

Event	Historic Geometry Scenario	Peak Difference (cfs)	Percent Change (%)	Arrival time difference (hr)	Peak Differnce (ft)	Percent Change (%)	Arrival time difference (hr)
August 2017	3040 - 5060	174.51	3.25	-0.8	0.12	0.53	-1.7
	5060 - 8090	-58.48	-1.05	0.2	0.06	0.27	-0.8
	8090 - Current	288.12	5.25	1.0	-0.05	-0.22	-0.5
	3040 - Current	404.15	7.52	0.3	0.13	0.58	-3.0
October 2017	3040 - 5060	775.92	8.46	-2.5	0.02	0.07	-2.0
	5060 - 8090	-256.95	-2.58	1.2	0.04	0.15	-2.2
	8090 - Current	1508.18	15.56	7.2	0.56	2.07	0.8
	3040 - Current	2027.15	22.09	5.8	0.62	2.30	-3.3
March 2016	3040 - 5060	312.77	2.09	-5.5	0.07	0.22	-3.8
	5060 - 8090	522.32	3.42	0.3	0.35	1.08	-0.5
	8090 - Current	1130.53	7.16	4.2	0.55	1.68	2.3
	3040 - Current	1965.62	13.15	-1.0	0.97	3.00	-2.0
August 2016	3040 - 5060	1135.19	2.96	2.0	0.07	0.16	-1.0
	5060 - 8090	268.82	0.68	-0.5	0.31	0.71	-2.5
	8090 - Current	3044.5	7.65	-2.0	0.61	1.39	-1.5
	3040 - Current	4448.51	11.59	-0.5	0.99	2.27	-5.0

The Amite River cross section 295071.9, just downstream of the confluence, shows an overall decrease in flow peak magnitude with slight delays in peak arrival time for older, more sinuous geometries compared to current (Figure 20). The August 2017 plot was especially interesting because unlike the other rainfall events, where the timing of the peaks coincided with one another on the Amite and Comite Rivers and a single, larger peak was seen once the rivers merged, the peak flow on the Comite River arrived at the confluence before the peak flow on the Amite River and resulted in a wider hydrograph with two smaller peaks (Figure 20a). This is consistent for all of the geometry scenarios and therefore not a product of channel planform geometry change, but instead a result of the rainfall distribution and timing. The peak stage hydrographs show overall decreases in peak magnitude and wider hydrographs, with the double peak for the August 2017 event again observed (Figure 21).

The percent change in flow and stage peaks are again the most notable for the March 2016 and August 2016 events, with the recent time periods also yielding significant results for the October 2017 event (Figure 22, Figure 22c). When comparing the percent change in peak flow and stage by historical planform geometry scenario, again there does not seem to be a direct correlation between the magnitude of loss in sinuosity along the two rivers and the magnitude of increase in flow and stage peak for every time period, although there is an overall loss of sinuosity and increase of flow peak (Figure 22, Figure 22d).

Similar to the Amite cross section upstream of the confluence, all of the storm events had an earlier arrival time for both stage and flow peaks the current scenario when comparing the cumulative time period (3040-current) (Table 6). The only cases that resulted in later peaks for the current were the March 2016 and October 2017 events between 8090 and current. The greatest

differences in arrival times for both stage and flow were seen for the largest event, August 2016, and a smaller October 2017 event.

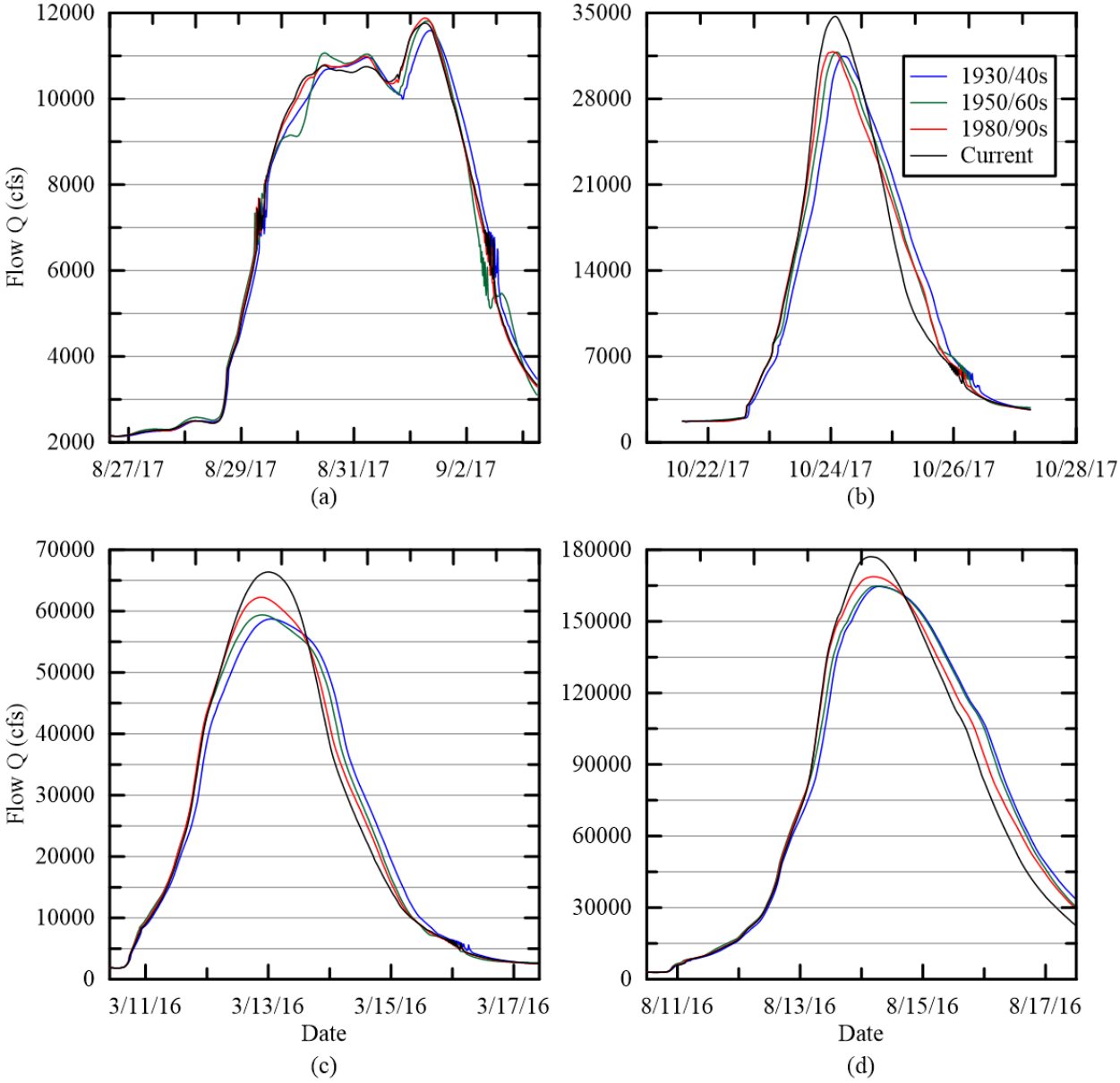

Figure 20. Flow hydrographs for Amite River 295071.9, the cross section directly downstream of the confluence for the four flow events (a.) August 2017, (b.) October 2017, (c.) March 2016, and (d.) August 2016.

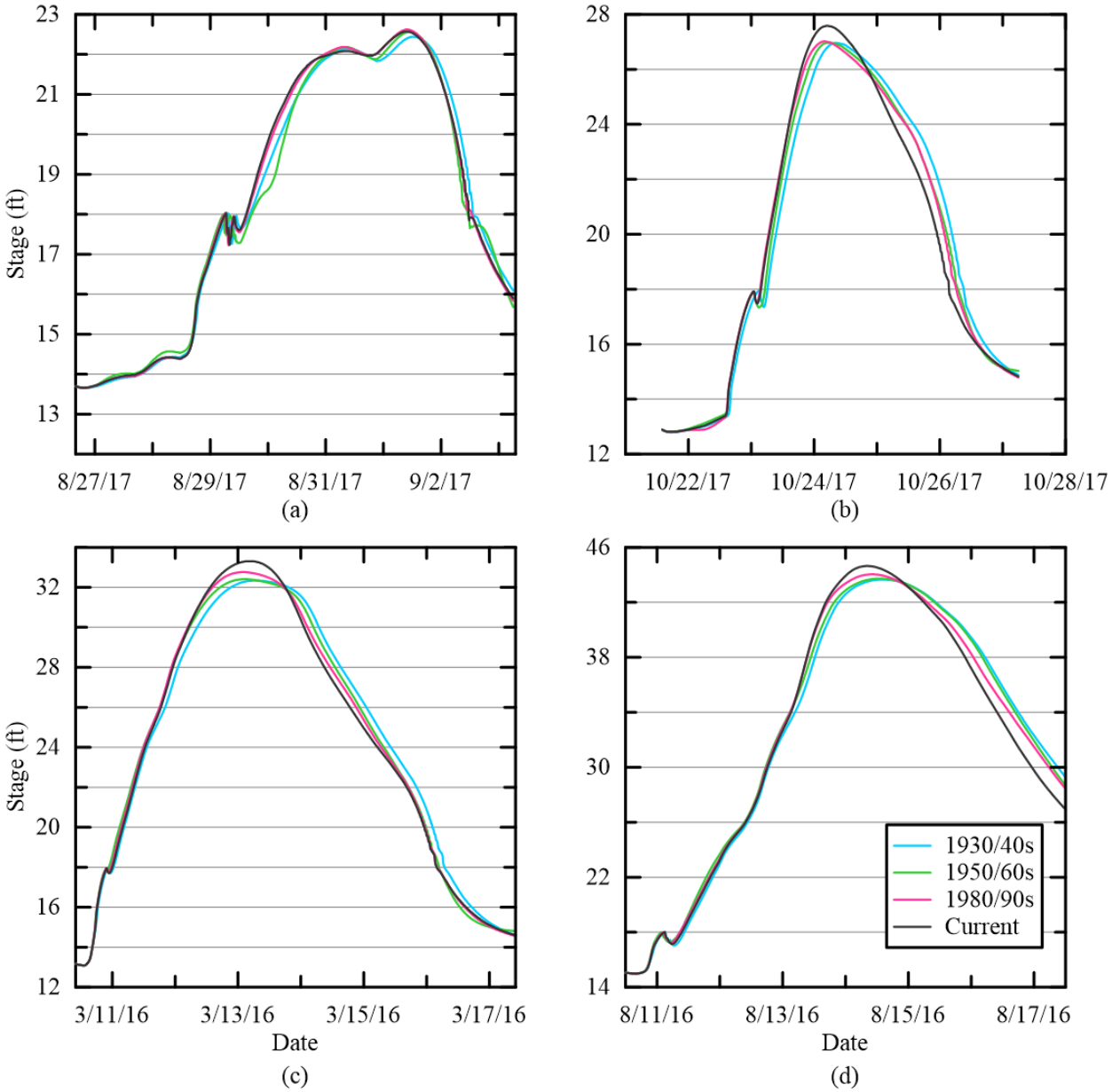

Figure 21. Stage hydrographs for Amite River 295071.9, the cross section directly downstream of the confluence for the four flow events (a.) August 2017, (b.) October 2017, (c.) March 2016, and (d.) August 2016.

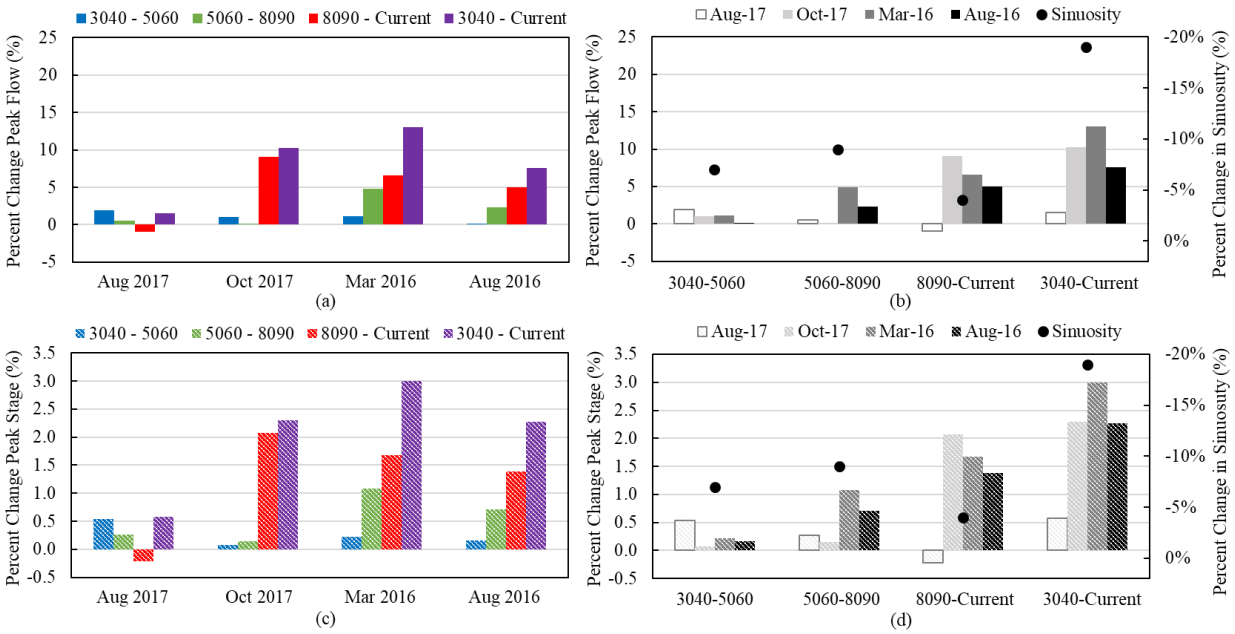

Figure 22. Percent change in (a.) flow, grouped into storm events, (b.) flow, grouped into differences between historical scenarios with the corresponding change in length/sinuosity, (c.) stage, grouped into storm events, (b.) stage, grouped into differences between historical scenarios with the corresponding change in length/sinuosity for Amite River 295071.9.

Table 6. Values for the difference in peak magnitude, percent change in peak magnitudes, and difference in arrival time for stage and flow for the four rainfall events between the geometry scenarios at Amite River cross section 295071.9.

Event	Historic Geometry Scenario	Peak Difference (cfs)	Percent Change (%)	Arrival time difference (hr)	Peak Differnce (ft)	Percent Change (%)	Arrival time difference (hr)
August 2017	3040 - 5060	224.4	1.94	-1.5	0.12	0.53	-1.6
	5060 - 8090	68.17	0.58	-0.7	0.06	0.27	-0.8
	8090 - Current	-116.64	-0.98	0.0	-0.05	-0.22	-0.5
	3040 - Current	175.93	1.52	-2.2	0.13	0.58	-3.0
October 2017	3040 - 5060	336.6	1.07	-2.3	0.02	0.07	-2.0
	5060 - 8090	24.08	0.08	-1.7	0.04	0.15	-2.2
	8090 - Current	2879.93	9.05	0.8	0.56	2.07	0.8
	3040 - Current	3240.61	10.30	-3.2	0.62	2.30	-3.3
March 2016	3040 - 5060	686.4	1.17	-3.5	0.07	0.22	-3.8
	5060 - 8090	2878.48	4.85	-0.5	0.35	1.08	-0.5
	8090 - Current	4106.26	6.59	2.8	0.55	1.68	2.3
	3040 - Current	7671.14	13.07	-1.2	0.97	3.00	-2.0
August 2016	3040 - 5060	137.5	0.08	-1.0	0.07	0.16	-1.0
	5060 - 8090	3897.2	2.37	-1.5	0.31	0.71	-2.5
	8090 - Current	8428.8	5.00	-1.0	0.61	1.39	-1.5
	3040 - Current	12463.5	7.57	-3.5	0.99	2.27	-5.0

CHAPTER 6. Discussion and Conclusions

6.1. Discussion

The Amite and Comite Rivers have decreased in length overall from the 1930s to today. The largest decrease is 13% on the portion of the Amite upstream of the confluence with the Comite from the 1930's to today. The Comite River decreased in length and sinuosity by 6% overall, and the Amite River downstream of the confluence decreased by only 1% overall. The changes can be linked to other occurrences within the basin such as development and sand and gravel mining and its impacts, but likely the most important take away from the presented length and sinuosity data is the temporal and spatial variability of the change. This has implications for the resultant flow routing seen in the basin because the spatially non uniform changes in length and sinuosity can result in additive or diminutive effects on the flow and stage peak as the water travels down the rivers. These spatially- and temporally-variable changes add to the complexity of the river basin and are one component that makes defining clear relationship and drawing conclusions a more challenging task.

There appears to be a relationship between the historical changes in planform geometry and the resulting stage and flow peak magnitudes and timing, although some inconsistencies arise. When comparing the cumulative time period (3040 to current), there has been a significant overall decrease in length and sinuosity on the Amite and Comite Rivers which corresponds to an overall increase in peak stage and flow magnitude and earlier peak arrival times. This is fairly consistent with what was found in a sensitivity analysis in Autin (1992) that estimated a 6 to 9.6-inch increase in stage at Denham Springs with a 20% reduction in river length in the Amite River. The results of this study show a 2 to 12-inch increase in stage given a 13% decrease in length along the Amite River with the greater impacts seen at greater magnitude flow events. Within the

intermediate time periods, there are cases where the trend of length and sinuosity change does not match with the trend seen in peak magnitude change. This alludes to the complexity of the study given the spatially- and temporally- variable changes in length and sinuosity over time and the use of variably distributed historical rainfall events. For instance, at the Comite cross section just upstream of the confluence, the October 2017 and August 2017 events arrive later in the current scenario, unlike what was seen in other storms and cross sections. This is due to the distribution of geometry changes in the basin because the 8090-current scenario actually had an increase in sinuosity and the rainfall for August and October 2017 passed through this portion of the river, causing a delay in arrival time compared to earlier conditions. Additionally, a possible explanation for why there was a consistent anomaly between the peak magnitudes and sinuosity between 8090 and current for all cross sections is that there could have been unknown errors in the model that caused the change in length and sinuosity for the 8090 scenario to not be properly represented. Finally, the percent change in flow is consistently greater than the percent change in stage so all events and all cross sections. This is explained by the rating curves "flattening out" as the flows continue to increase and the stages increase by much smaller increments once the flow is out of banks. This is further validated because the smaller, within-bank events do not show as large of a difference between the magnitudes of change between flow and stage.

While the results of this study cannot prove a strong, consistent direct link between the changing in planform geometry and a positive or negative correlation with peak stage and flow or arrival time, several interesting patterns were observed in regards to the flow events. According to the percent changes in flow and stage peak magnitude, the impacts of the decreases in channel length and sinuosity were most realized in the larger flow events, in this case March 2016 and August 2016, on the Amite River both upstream and downstream of the confluence. The March

and August 2016 events also had notable impacts on the percent change in peak stage and flow on the Comite River, with the October 2017 event also eliciting a strong response. The March 2016 and August 2016 were expected to elicit notable responses in stage and flow simply due to the amount of rain that fell and would be routed down the rivers. Both events had significant rainfall in the middle to upper portion of the basin, allowing more water to pass through the Amite and Comite Rivers upstream of the confluence, which is where the changes in planform geometry occurred. However, given the sheer magnitude of the August 2016 event and the amount of water that was in the floodplain, there was a question whether the flow would simply overwhelm the river in general and the responses of changes in planform geometry would not be noticed. August 2017 was not expected to result in major changes in the peak flow and stage because it was a much smaller event and the rainfall fell mostly in the lower portion of the basin so much of the rainfall was not routed through the reaches that experience the most change. October 2017 was a smaller event, however, the majority of the rain fell on the upper portion of both rivers and therefore would be routed through the reaches that endured the most change. October 2017 is the event that would give the best picture of how a bankfull flow would be impacted by these changes in length and sinuosity and it is therefore interesting that in several cases the percent change in stage and flow was fairly comparable with the much larger events. Relative to the flow, the changes were overall most apparent with the March 2016 and then the October 2017 event, followed by the August 2016 event, which was expected given the nature of the events. Again, the storm events that were used were measured, historical rainfall data that had varying spatial distributions. August 2017 resulted in 1-year return period flows throughout the basin, October 2017 resulted in 1.4 to 2.4-year return period flows, March 2016 resulted in 2.8 to 6-year return period flows, and August 2016 resulted in 100 to greater than 500-year return period flows.

6.2. Conclusions and Future Work

This thesis investigated the historical changes in planform geometry on the Amite and Comite Rivers from 1930s to the present and used a HEC-RAS model to simulate the resulting impacts on flood routing for four rainfall events. The Amite and Comite Rivers have both experienced an overall decrease in length and sinuosity from the 1930s to present at varying spatial and temporal degrees. The model results show an overall increase in peak flow and stage magnitude corresponding to the overall decrease in river length and sinuosity, with slightly variable results for the intermediate time periods. The March 2016 event, a 2.8- to 6-yr flow event, appeared to show the greatest percent change in stage and flow across the rivers, given the magnitude of the event and the distribution of the rainfall. October 2017 and August 2016, 1.5-yr and greater than 500-yr return period flow events respectively, elicited the next greatest response in percent change in peak flow and stage. August 2017, a 1-year return period flow event, brought about little change in peak flow and stages due to the small magnitude and rainfall distribution not covering the reaches that experienced change. The variable changes in river planform geometry and the non-uniform distribution of rainfall in the events used add to the complexity of the study and varying trends observed.

While the objective of this thesis is not to quantify the difference in flood *risk*, the overall trends of narrower hydrographs with higher peak flow and stage values due to the shortening and straightening of the Amite and Comite Rivers does pose a greater threat of flooding the areas surrounding the river. A narrower hydrograph with a higher peak would result in a greater area flooded for a shorter amount of time, as discussed in the literature review, which in terms of financial loss would be a greater impact compared to fewer areas flooded for slightly longer amounts of time. The methodology chosen for this study is not intended to quantify the difference

in flooded area, however, it does have implications for such a study being conducted in the future and being related to flood risk and financial loss.

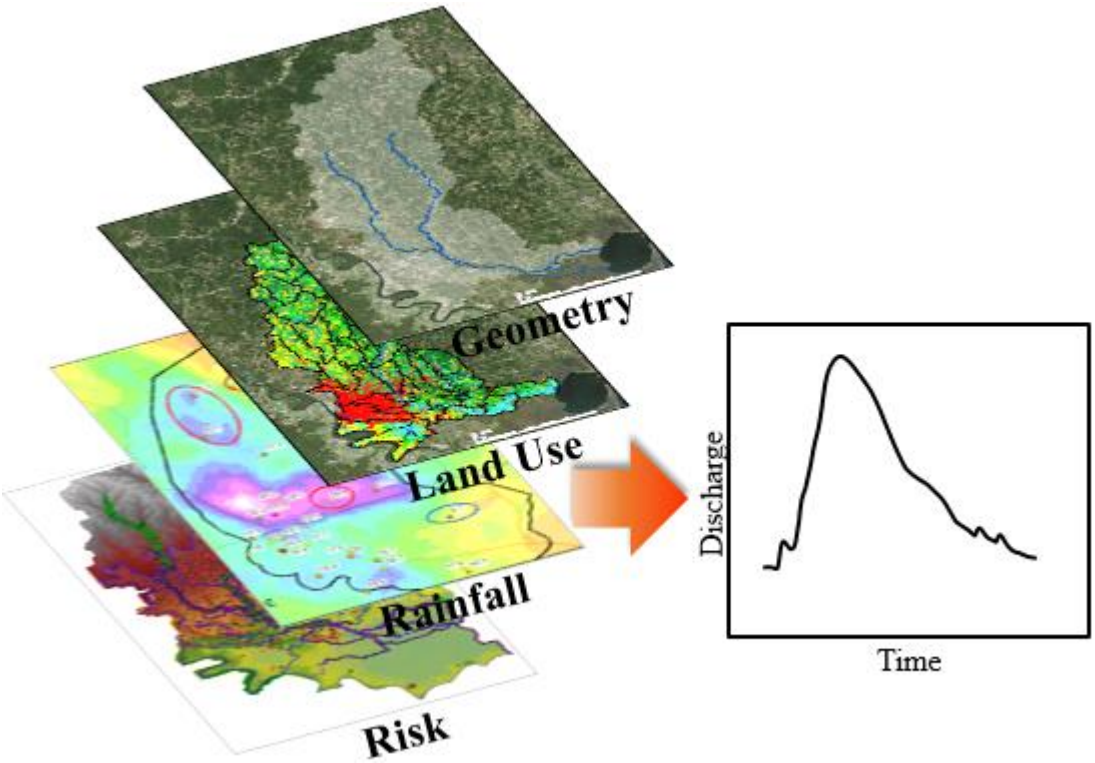

Figure 23. Conceptual figure showing several of the variables that are studied when considering the changes in a basin and the impacts these changes have on flood routing.

River geometry is only one factor impacting the magnitude and timing of flood events. Other factors that were not accounted for are the changes in bathymetry and the areas of aggradation and degradation that have occurred within the basin. Additional facets include changing magnitudes of rainfall events experienced and how land use change has impacted runoff flowing into the rivers. Results from this study will be coupled and compared to complementary projects, focused on spatial and temporal changes in land use and precipitation events, to better understand the driving variables impacting the stages, discharges, and flood risk, shown in the conceptual figure (Figure *23*). The implication of this study, and the related ongoing work, relates to better understanding flooding in this basin, how impacts and disturbances have changed the flooding dynamics over

time, and how projects can be used to mitigate flooding moving forward. This study has highlighted that this basin, and all river basins, are complex systems and the hydrographs within the rivers and subsequent out-of-banks flooding are driven by a multitude of variables. The variable discussed within this study was river length and sinuosity, but more can be investigated around the river channel change such as geomorphic alterations and impacts to the roughness values along the reaches. More work is needed to further test the response flood routing has to the geometry impacts such as utilizing uniform rainfall distributions rather than variable, historic events. This would simplify the inputs and allow additional detailed study of the flood routing responses.

REFERENCES

Autin, W. J. (1992). *Govenor's Interagency Task Force on Flood Preventaion and Mitigation.* Baton Rouge: Department of Natural Resources Louisiana Geological Survey.

Autin, W. J., & Fontana, C. M. (1980). Preliminary Observation of Modern Point Bar Facies, Amite River, Louisiana. *The Gulf Coast Association of Geological Societies Transactions, 30,* pp. 259-262. Corpus Christi, Texas.

Bedient, P. B., Huber, W. C., & Vieux, B. E. (2013). *Hydrology and Floodplain Analysis* (5th ed.). Upper Saddle River, NJ: Pearson Education Inc.

Brown, V. M., Keim, B. D., Kappel, W. D., Hultstrand, D. M., Peyrefitte Jr., A. G., Black, A. W., . . . Muhlestein, G. A. (2020). How Rare Was the August 2016 South-Central Louisiana Heavy Rainfall Event? *Journal of Hydrometeorology, 21*(4), 773-790. doi:10.1175/JHM-D-19-0225.1

Brunner, G. (2016). *HEC-RAS, River Analysis System Hydraulic Reference Manual.* Davis, CA: Army Corps of Engineers Hydraulic Engineering Center. Retrieved from https://www.hec.usace.army.mil/software/hec-ras/documentation/HEC-RAS%205.0%20Reference%20Manual.pdf

Campbell, K. L., Kumar, S., & Johnson, H. P. (1972). Stream Straightening Effects on Flood-Runoff Characteristics. *Transactions of the American Society of Agricultural Engineers, 15*, 94-98.

Davis, A. H. (2009). *Floodplain Mining and Channel Planform Change Along the Amite River, Louisiana:1976 - 1998.* Gainsville, Florida: Masters Thesis, University of Florida.

Deng, Z., & Patil, A. A. (2011). Assessment of water quality variation in Amite River watershed under changing climate and land use. *Water Quality: Current Trends and Expected Climate Change Impacts Water Quality: Current Trends and Expected Climate Change Impacts (Proceedings of symposium H04 held during IUGG2011)* (pp. 20-25). Melbourne, Australia: International Association of Hydrilogical Sciences.

Dewberry Engineers Inc. (2019). *Amite River Basin Numerical Model* . New Orleans, LA.

Doyle, M. W., Shields, D., Boyd, K. F., Skidmore, P. B., & Dominick, D. (2007). Channel-Forming Discharge Selection in River Restoration Design. *Journal of Hydraulic Engineering, 1337*, 831-837.

Emmer, R. E. (2003). *A Disaster That Didn't Have to Happen: The East Baton Rouge Parish Flood of 2001.* Baton Rouge, LA: Coastal Environments, Inc.

Federal Emergency Management Agency (FEMA). (2017). *Louisiana Watershed Resiliency Study Developed Following the March and Augsut 2016 Floods.* Baton Rouge.

Ferguson, R. I. (1986). Hydraulics and Hydraulic Geometry. *Progress in Physical Geography: Earth and Environment, 10*(1), 1-31.

Gleason, C. J. (2015). Hydraulic Geometry of Natural Rivers: A Review and Future Directions. *Progress in Physical Geography, 39*(3), 337-360.

Gulf Engineers and Consultants. (2015). *Amite River Basin Floodplain Management Plan.* Baton Rouge, LA: Amite River Basin Drainage and Water Conservation District .

Hood, R. D., Patrick, D. M., & Corcoran, M. K. (2007). *Fluvial Instability and Channel Degradation of Amite River and its Tributaries, Southwest Mississippi and Southeast Louisiana.* Vicksburg, MS: U.S. Army Engineer Research and Development Center.

Julien, P. Y. (2018). *River Mechanics.* Cambridge, United Kingdom: Cambridge University Press.

Lauer, J. W. (2006). Channel Planform Statistics Toolbox. Minneapolis, MN: National Center for Earth-surface Dynamics. Retrieved from http://www.nced.umn.edu/: https://repository.nced.umn.edu/browser.php?current=author&author=37&dataset_id=15

Lee, H.-Y., Fu, D.-T., & Song, M.-H. (1993). Migration of Rectangular Mining Pit Composed of Uniform Sediments. *Journal of Hydraulic Engineering, 119*(1), 64-80.

Leopold, L. B., & Maddock Jr., T. (1953). *The Hydraulic Geometry of Stream Channels and Some Physiographic Implications.* Washington D.C.: United State Government Printing Office.

Little, C. D. (2011). *Amite River Field Investigation and Gemorphic Assessment.* Vicksburg, MS: USACE ERDC Coastal & Hydraulica Laboratory.

Lyles, J. E. (1999). *Amite River Sand and Gravel Mine Reclemation Demonstration Project.* Baton Rouge, LA: LA Department of Environmental Quality - Office of Environmental Assessement, Nonpoint Source Pollution Unit.

Marsh, G. P. (1864). *Man and nature: Physical Geography as Modified by Human Action.* New York: Charles Scribner.

Mishra, P. K., & Deng, Z.-Q. (2009). Sediment TMDL Development for the Amite River. *Water Resourse Management, 23*(5), 839-852. doi:10.1007/s11269-008-9302-4

Mossa, J., & McLean, M. (1997). Channel Planform and Land Cover Changes on a Mined River Floodplain. *Applied Geography, 17*(1), 43-54.

Neal, J. C., Odoni, N. A., Trigg, M. A., Freer, J. E., Garcia-Pintado, J., Mason, D. C., & Bates, P. D. (2015). Efficient incorporation of channel cross-section geometry uncertainty into regional and global scale flood inundation models. *Journal of Hydrology, 529*, 169-183.

Phillips, J. D. (1990). The Instabilty of Hydraulic Geometry. *Water Resources Resarch, 26*(4), 739-744.

Schoof, R. (1980). Environmental Impact of Channel Modification. *Water Resources Bulletin, 16*, 697-701.

Sholtes, J. S., & Doyle, M. W. (2011). Effect of Channel Restoration on Flood Wave Attenuation. *Journal of Hydraulic Engineering, 137*, 196-208.

Simon, A. (1994). *Gradation Processes and Channel Evolution in Modified West Tennessee Streams: Process, Response, and Form.* U.S. Geological Survey Professional Paper 1470.

Singh, V. P. (2003). On the Theories of Hydraulic Geometry. *International Journal of Sediment Research, 18*(3), 196-218.

Stall, J. B., & Yang, C. T. (1970). *Hydraulic Geometry of 12 Selected Stream Systems of the United States.* Urbana, Illinois: University of Illinois Water Resource Center.

Step, S. b. (1999). *Impact Assessment of Instream Management Practices on Channel Morphology.* Waterbury, Vermont: Vermont Department of Environmental Conservation.

Sturm, T. W. (2001). *Open Channel Hydraulics.* Boston: McGraw-Hill.

U.S. Army Corps of Engineers. (1955). *Survey of Amite River and Tributaries Louisiana.* New Orleans, LA: USACE New Orleans Disctrict.

U.S. Geological Survey and U.S. Department of Agriculture, Natural Resource Conservation Service. (2013). , Federal Standards and Procedures for the National Watershed Boundary Dataset (WBD) (4 ed.). In *U.S. Geological Survey Techniques and Methods Book 11, Collection and Delineation of Spatial Data* (p. 63). Retrieved from http://pubs.usgs.gov/tm/tm11a3/

Watson, K. M., Storm, J. B., Breaker, B. K., & Rose, C. E. (2017). *Characterization of Peak Streamflows and Flood Inundation of Selected Areas in Louisiana from the August 2016 Flood.* Reston, VA: U.S. Geological Survey Scientific Investigations Report. doi:https://doi.org/10.3133/sir20175005

Wohl, E. (2006). Human Impacts to Mountain Streams. *Geomorphology, 76*, 217-248.

Wyzga, B. (1997). Methods for studying the response of flood flows to channel change. *Journal of Hydrology, 198*, 271-288.

Wyzga, B. (2001). Impact of the Channelization-Induced Incision of the Skawa and Wisloka Rivers, Southern Poland, on the Conditions of Overbank Deposition. *Regulated Rivers: Research anf Management, 17*, 85-100.

Yang, L., Smith, J. A., Wright, D. B., Baech, M. L., Villarani, G., Tian, F., & Hu, H. (2013). Urbanization and Climate Change: An Examination of Nonstationarities in Urban Flooding. *Journal of Hydrometeorology, 14*, 1791-1808.

Zhang, W., Villarini, G., Vencchi, G. A., & Smith, J. A. (2018). Urbanization exacerbated the rainfall and flooding caused by hurrican Harvey in Houston. *Nature, 563*, 384-398.

VITA

Kathleen Eubanks Harris was born to Robert and Salvatrice Eubanks in Harahan, LA. Just upstream of New Orleans, she grew up riding her bike on the levee and looking over and appreciating the Mississippi River. She has always enjoyed being from Louisiana and learning about the problems that the state faces because of its complicated relationship with water. After obtaining her B.S. in Bioenvironmental Sciences from Texas A&M University in 2016 with a concentration in coastal ecology, she pivoted to engineering through the Coastal and Ecological Engineering Master's program at LSU. She began working at the U.S. Army Corps of Engineers Research and Development Center (ERDC) in Vicksburg, MS in May, 2020 as a Research Civil Engineer (Hydraulics) in the Coastal and Hydraulics Lab and anticipates graduating in December 2020 with her M.S. in Coastal and Ecological Engineering. She has passed her Fundamentals of Engineering exam and looks forward to pursing her Professional Engineering license in the coming years. She currently resides in Vicksburg, MS with her husband Brain and their three cats as they eagerly await the arrival of their first child, a daughter, in October 2020.